Eur. Phys. J. C 18, 203–228 (2000)
Digital Object Identifier (DOI) 10.1007/s100520000528

THE EUROPEAN PHYSICAL JOURNAL C

Charged and identified particles in the hadronic decay of W bosons and in $e^+e^- \to q\bar{q}$ from 130 to 200 GeV

The DELPHI Collaboration

P. Abreu[22], W. Adam[52], T. Adye[38], P. Adzic[12], Z. Albrecht[18], T. Alderweireld[2], G.D. Alekseev[17], R. Alemany[51], T. Allmendinger[18], P.P. Allport[23], S. Almehed[25], U. Amaldi[9,29], N. Amapane[47], S. Amato[49], E.G. Anassontzis[3], P. Andersson[46], A. Andreazza[9], S. Andringa[22], N. Anjos[22], P. Antilogus[26], W-D. Apel[18], Y. Arnoud[9], B. Åsman[46], J-E. Augustin[26], A. Augustinus[9], P. Baillon[9], A. Ballestrero[47], P. Bambade[20], F. Barao[22], G. Barbiellini[48], R. Barbier[26], D.Y. Bardin[17], G. Barker[18], A. Baroncelli[40], M. Battaglia[16], M. Baubillier[24], K-H. Becks[54], M. Begalli[6], A. Behrmann[54], P. Beilliere[8], Yu. Belokopytov[9], K. Belous[44], N.C. Benekos[33], A.C. Benvenuti[5], C. Berat[15], M. Berggren[24], D. Bertrand[2], M. Besancon[41], M. Bigi[47], M.S. Bilenky[17], M-A. Bizouard[20], D. Bloch[10], H.M. Blom[32], M. Bonesini[29], M. Boonekamp[41], P.S.L. Booth[23], G. Borisov[20], C. Bosio[43], O. Botner[50], E. Boudinov[32], B. Bouquet[20], C. Bourdarios[20], T.J.V. Bowcock[23], I. Boyko[17], I. Bozovic[12], M. Bozzo[14], M. Bracko[45], P. Branchini[40], R.A. Brenner[50], P. Bruckman[9], J-M. Brunet[8], L. Bugge[34], T. Buran[34], B. Buschbeck[52], P. Buschmann[54], S. Cabrera[51], M. Caccia[28], M. Calvi[29], T. Camporesi[9], V. Canale[39], F. Carena[9], L. Carroll[23], C. Caso[14], M.V. Castillo Gimenez[51], A. Cattai[9], F.R. Cavallo[5], V. Chabaud[9], M. Chapkin[44], Ph. Charpentier[9], P. Checchia[37], G.A. Chelkov[17], R. Chierici[47], P. Chliapnikov[9,44], P. Chochula[7], V. Chorowicz[26], J. Chudoba[31], K. Cieslik[19], P. Collins[9], R. Contri[14], E. Cortina[51], G. Cosme[20], F. Cossutti[9], M. Costa[51], H.B. Crawley[1], D. Crennell[38], S. Crepe[15], G. Crosetti[14], J. Cuevas Maestro[35], S. Czellar[16], M. Davenport[9], W. Da Silva[24], G. Della Ricca[48], P. Delpierre[27], N. Demaria[9], A. De Angelis[48], W. De Boer[18], C. De Clercq[2], B. De Lotto[48], A. De Min[37], L. De Paula[49], H. Dijkstra[9], L. Di Ciaccio[9,39], J. Dolbeau[8], K. Doroba[53], M. Dracos[10], J. Drees[54], M. Dris[33], A. Duperrin[26], J-D. Durand[9], G. Eigen[4], T. Ekelof[50], G. Ekspong[46], M. Ellert[50], M. Elsing[9], J-P. Engel[10], M. Espirito Santo[9], G. Fanourakis[12], D. Fassouliotis[12], J. Fayot[24], M. Feindt[18], A. Ferrer[51], E. Ferrer-Ribas[20], F. Ferro[14], S. Fichet[24], A. Firestone[1], U. Flagmeyer[54], H. Foeth[9], E. Fokitis[33], F. Fontanelli[14], B. Franek[38], A.G. Frodesen[4], R. Fruhwirth[52], F. Fulda-Quenzer[20], J. Fuster[51], A. Galloni[23], D. Gamba[47], S. Gamblin[20], M. Gandelman[49], C. Garcia[51], C. Gaspar[9], M. Gaspar[49], U. Gasparini[37], Ph. Gavillet[9], E.N. Gazis[33], D. Gele[10], T. Geralis[12], N. Ghodbane[26], I. Gil[51], F. Glege[54], R. Gokieli[9,53], B. Golob[9,45], G. Gomez-Ceballos[42], P. Goncalves[22], I. Gonzalez Caballero[42], G. Gopal[38], L. Gorn[1], Yu. Gouz[44], V. Gracco[14], J. Grahl[1], E. Graziani[40], P. Gris[41], G. Grosdidier[20], K. Grzelak[53], J. Guy[38], C. Haag[18], F. Hahn[9], S. Hahn[54], S. Haider[9], A. Hallgren[50], K. Hamacher[54], J. Hansen[34], F.J. Harris[36], F. Hauler[18], V. Hedberg[9,25], S. Heising[18], J.J. Hernandez[51], P. Herquet[2], H. Herr[9], T.L. Hessing[36], J.-M. Heuser[54], E. Higon[51], S-O. Holmgren[46], P.J. Holt[36], S. Hoorelbeke[2], M. Houlden[23], J. Hrubec[52], M. Huber[18], K. Huet[2], G.J. Hughes[23], K. Hultqvist[9,46], J.N. Jackson[23], R. Jacobsson[9], P. Jalocha[19], R. Janik[7], Ch. Jarlskog[25], G. Jarlskog[25], P. Jarry[41], B. Jean-Marie[20], D. Jeans[36], E.K. Johansson[46], P. Jonsson[26], C. Joram[9], P. Juillot[10], L. Jungermann[18], F. Kapusta[24], K. Karafasoulis[12], S. Katsanevas[26], E.C. Katsoufis[33], R. Keranen[18], G. Kernel[45], B.P. Kersevan[45], Yu. Khokhlov[44], B.A. Khomenko[17], N.N. Khovanski[17], A. Kiiskinen[16], B. King[23], A. Kinvig[23], N.J. Kjaer[9], O. Klapp[54], H. Klein[9], P. Kluit[32], P. Kokkinias[12], V. Kostioukhine[44], C. Kourkoumelis[3], O. Kouznetsov[17], M. Krammer[52], E. Kriznic[45], Z. Krumstein[17], P. Kubinec[7], J. Kurowska[53], K. Kurvinen[16], J.W. Lamsa[1], D.W. Lane[1], V. Lapin[44], J-P. Laugier[41], R. Lauhakangas[16], G. Leder[52], F. Ledroit[15], V. Lefebure[2], L. Leinonen[46], A. Leisos[12], R. Leitner[31], J. Lemonne[2], G. Lenzen[54], V. Lepeltier[20], T. Lesiak[19], M. Lethuillier[41], J. Libby[36], W. Liebig[54], D. Liko[9], A. Lipniacka[9,46], I. Lippi[37], B. Loerstad[25], J.G. Loken[36], J.H. Lopes[49], J.M. Lopez[42], R. Lopez-Fernandez[15], D. Loukas[12], P. Lutz[41], L. Lyons[36], J. MacNaughton[52], J.R. Mahon[6], A. Maio[22], A. Malek[54], T.G.M. Malmgren[46], S. Maltezos[33], V. Malychev[17], F. Mandl[52], J. Marco[42], R. Marco[42], B. Marechal[49], M. Margoni[37], J-C. Marin[9], C. Mariotti[9], A. Markou[12], C. Martinez-Rivero[20], S. Marti i Garcia[9], J. Masik[13], N. Mastroyiannopoulos[12], F. Matorras[42], C. Matteuzzi[29], G. Matthiae[39], F. Mazzucato[37], M. Mazzucato[37], M. Mc Cubbin[23], R. Mc Kay[1], R. Mc Nulty[23], G. Mc Pherson[23], C. Meroni[28], Z. Metreveli[9], W.T. Meyer[1], A. Miagkov[44], E. Migliore[9], L. Mirabito[26], W.A. Mitaroff[52], U. Mjoernmark[25], T. Moa[46], M. Moch[18], R. Moeller[30], K. Moenig[9,11], M.R. Monge[14], D. Moraes[49], X. Moreau[24], P. Morettini[14], G. Morton[36], U. Mueller[54], K. Muenich[54], M. Mulders[32], C. Mulet-Marquis[15], R. Muresan[25], W.J. Murray[38], B. Muryn[19], G. Myatt[36], T. Myklebust[34], F. Naraghi[15], M. Nassiakou[12], F.L. Navarria[5], K. Nawrocki[53], P. Negri[29], N. Neufeld[9], R. Nicolaidou[41], B.S. Nielsen[30], P. Niezurawski[53], M. Nikolenko[10,17], V. Nomokonov[16], A. Nygren[25], V. Obraztsov[44], A.G. Olshevski[17], A. Onofre[22], R. Orava[16], G. Orazi[10], K. Osterberg[16], A. Ouraou[41], A. Oyanguren[51], M. Paganoni[29], S. Paiano[5], R. Pain[24], R. Paiva[22], J. Palacios[36], H. Palka[19], Th.D. Papadopoulou[9,33], L. Pape[9], C. Parkes[9], F. Parodi[14], U. Parzefall[23],

A. Passeri[40], O. Passon[54], T. Pavel[25], M. Pegoraro[37], L. Peralta[22], M. Pernicka[52], A. Perrotta[5], C. Petridou[48], A. Petrolini[14], H.T. Phillips[38], F. Pierre[41], M. Pimenta[22], E. Piotto[28], T. Podobnik[45], M.E. Pol[6], G. Polok[19], P. Poropat[48], V. Pozdniakov[17], P. Privitera[39], N. Pukhaeva[17], A. Pullia[29], D. Radojicic[36], S. Ragazzi[29], H. Rahmani[33], J. Rames[13], P.N. Ratoff[21], A.L. Read[34], P. Rebecchi[9], N.G. Redaelli[29], M. Regler[52], J. Rehn[18], D. Reid[32], P. Reinertsen[4], R. Reinhardt[54], P.B. Renton[36], L.K. Resvanis[3], F. Richard[20], J. Ridky[13], G. Rinaudo[47], I. Ripp-Baudot[10], O. Rohne[34], A. Romero[47], P. Ronchese[37], E.I. Rosenberg[1], P. Rosinsky[7], P. Roudeau[20], T. Rovelli[5], Ch. Royon[41], V. Ruhlmann-Kleider[41], A. Ruiz[42], H. Saarikko[16], Y. Sacquin[41], A. Sadovsky[17], G. Sajot[15], J. Salt[51], D. Sampsonidis[12], M. Sannino[14], Ph. Schwemling[24], B. Schwering[54], U. Schwickerath[18], F. Scuri[48], P. Seager[21], Y. Sedykh[17], A.M. Segar[36], N. Seibert[18], R. Sekulin[38], R.C. Shellard[6], M. Siebel[54], L. Simard[41], F. Simonetto[37], A.N. Sisakian[17], G. Smadja[26], O. Smirnova[25], G.R. Smith[38], O. Solovianov[44], A. Sopczak[18], R. Sosnowski[53], T. Spassov[22], E. Spiriti[40], S. Squarcia[14], C. Stanescu[40], S. Stanic[45], M. Stanitzki[18], K. Stevenson[36], A. Stocchi[20], J. Strauss[52], R. Strub[10], B. Stugu[4], M. Szczekowski[53], M. Szeptycka[53], T. Tabarelli[29], A. Taffard[23], F. Tegenfeldt[50], F. Terranova[29], J. Thomas[36], J. Timmermans[32], N. Tinti[5], L.G. Tkatchev[17], M. Tobin[23], S. Todorova[9], A. Tomaradze[2], B. Tome[22], A. Tonazzo[9], L. Tortora[40], P. Tortosa[51], G. Transtromer[25], D. Treille[9], G. Tristram[8], M. Trochimczuk[53], C. Troncon[28], M-L. Turluer[41], I.A. Tyapkin[17], P. Tyapkin[25], S. Tzamarias[12], O. Ullaland[9], V. Uvarov[44], G. Valenti[9,5], E. Vallazza[48], P. Van Dam[32], W. Van den Boeck[2], J. Van Eldik[9,32], A. Van Lysebetten[2], N. van Remortel[2], I. Van Vulpen[32], G. Vegni[28], L. Ventura[37], W. Venus[38,9], F. Verbeure[2], P. Verdier[26], M. Verlato[37], L.S. Vertogradov[17], V. Verzi[28], D. Vilanova[41], L. Vitale[48], E. Vlasov[44], A.S. Vodopyanov[17], G. Voulgaris[3], V. Vrba[13], H. Wahlen[54], C. Walck[46], A.J. Washbrook[23], C. Weiser[9], D. Wicke[9], J.H. Wickens[2], G.R. Wilkinson[36], M. Winter[10], M. Witek[19], G. Wolf[9], J. Yi[1], O. Yushchenko[44], A. Zalewska[19], P. Zalewski[53], D. Zavrtanik[45], E. Zevgolatakos[12], N.I. Zimin[17,25], A. Zintchenko[17], Ph. Zoller[10], G.C. Zucchelli[46], G. Zumerle[37]

[1] Department of Physics and Astronomy, Iowa State University, Ames IA 50011-3160, USA
[2] Physics Department, Univ. Instelling Antwerpen, Universiteitsplein 1, 2610 Antwerpen, Belgium
and IIHE, ULB-VUB, Pleinlaan 2, 1050 Brussels, Belgium
and Faculté des Sciences, Univ. de l'Etat Mons, Av. Maistriau 19, 7000 Mons, Belgium
[3] Physics Laboratory, University of Athens, Solonos Str. 104, 10680 Athens, Greece
[4] Department of Physics, University of Bergen, Allégaten 55, 5007 Bergen, Norway
[5] Dipartimento di Fisica, Università di Bologna and INFN, Via Irnerio 46, 40126 Bologna, Italy
[6] Centro Brasileiro de Pesquisas Físicas, rua Xavier Sigaud 150, 22290 Rio de Janeiro, Brazil
and Depto. de Física, Pont. Univ. Católica, C.P. 38071 22453 Rio de Janeiro, Brazil
and Inst. de Física, Univ. Estadual do Rio de Janeiro, rua São Francisco Xavier 524, Rio de Janeiro, Brazil
[7] Comenius University, Faculty of Mathematics and Physics, Mlynska Dolina, 84215 Bratislava, Slovakia
[8] Collège de France, Lab. de Physique Corpusculaire, IN2P3-CNRS, 75231 Paris Cedex 05, France
[9] CERN, CH-1211 Geneva 23, Switzerland
[10] Institut de Recherches Subatomiques, IN2P3 - CNRS/ULP - BP20, 67037 Strasbourg Cedex, France
[11] Now at DESY-Zeuthen, Platanenallee 6, 15735 Zeuthen, Germany
[12] Institute of Nuclear Physics, N.C.S.R. Demokritos, P.O. Box 60228, 15310 Athens, Greece
[13] FZU, Inst. of Phys. of the C.A.S. High Energy Physics Division, Na Slovance 2, 180 40, Praha 8, Czech Republic
[14] Dipartimento di Fisica, Università di Genova and INFN, Via Dodecaneso 33, 16146 Genova, Italy
[15] Institut des Sciences Nucléaires, IN2P3-CNRS, Université de Grenoble 1, 38026 Grenoble Cedex, France
[16] Helsinki Institute of Physics, HIP, P.O. Box 9, 00014 Helsinki, Finland
[17] Joint Institute for Nuclear Research, Dubna, Head Post Office, P.O. Box 79, 101 000 Moscow, Russian Federation
[18] Institut für Experimentelle Kernphysik, Universität Karlsruhe, Postfach 6980, 76128 Karlsruhe, Germany
[19] Institute of Nuclear Physics and University of Mining and Metalurgy, Ul. Kawiory 26a, 30055 Krakow, Poland
[20] Université de Paris-Sud, Lab. de l'Accélérateur Linéaire, IN2P3-CNRS, Bât. 200, 91405 Orsay Cedex, France
[21] School of Physics and Chemistry, University of Lancaster, Lancaster LA1 4YB, UK
[22] LIP, IST, FCUL - Av. Elias Garcia, 14-1^{o}, PT-1000 Lisboa Codex, Portugal
[23] Department of Physics, University of Liverpool, P.O. Box 147, Liverpool L69 3BX, UK
[24] LPNHE, IN2P3-CNRS, Univ. Paris VI et VII, Tour 33 (RdC), 4 place Jussieu, 75252 Paris Cedex 05, France
[25] Department of Physics, University of Lund, Sölvegatan 14, 223 63 Lund, Sweden
[26] Université Claude Bernard de Lyon, IPNL, IN2P3-CNRS, 69622 Villeurbanne Cedex, France
[27] Univ. d'Aix - Marseille II - CPP, IN2P3-CNRS, 13288 Marseille Cedex 09, France
[28] Dipartimento di Fisica, Università di Milano and INFN-MILANO, Via Celoria 16, 20133 Milan, Italy
[29] Dipartimento di Fisica, Univ. di Milano-Bicocca and INFN-MILANO, Piazza delle Scienze 2, 20126 Milan, Italy
[30] Niels Bohr Institute, Blegdamsvej 17, 2100 Copenhagen Ø, Denmark
[31] IPNP of MFF, Charles Univ., Areal MFF, V Holesovickach 2, 180 00, Praha 8, Czech Republic
[32] NIKHEF, Postbus 41882, 1009 DB Amsterdam, The Netherlands
[33] National Technical University, Physics Department, Zografou Campus, 15773 Athens, Greece
[34] Physics Department, University of Oslo, Blindern, 1000 Oslo 3, Norway
[35] Dpto. Fisica, Univ. Oviedo, Avda. Calvo Sotelo s/n, 33007 Oviedo, Spain
[36] Department of Physics, University of Oxford, Keble Road, Oxford OX1 3RH, UK

[37] Dipartimento di Fisica, Università di Padova and INFN, Via Marzolo 8, 35131 Padua, Italy
[38] Rutherford Appleton Laboratory, Chilton, Didcot OX11 OQX, UK
[39] Dipartimento di Fisica, Università di Roma II and INFN, Tor Vergata, 00173 Rome, Italy
[40] Dipartimento di Fisica, Università di Roma III and INFN, Via della Vasca Navale 84, 00146 Rome, Italy
[41] DAPNIA/Service de Physique des Particules, CEA-Saclay, 91191 Gif-sur-Yvette Cedex, France
[42] Instituto de Fisica de Cantabria (CSIC-UC), Avda. los Castros s/n, 39006 Santander, Spain
[43] Dipartimento di Fisica, Università degli Studi di Roma La Sapienza, Piazzale Aldo Moro 2, 00185 Rome, Italy
[44] Inst. for High Energy Physics, Serpukov P.O. Box 35, Protvino, (Moscow Region), Russian Federation
[45] J. Stefan Institute, Jamova 39, 1000 Ljubljana, Slovenia and Laboratory for Astroparticle Physics, Nova Gorica Polytechnic, Kostanjeviska 16a, 5000 Nova Gorica, Slovenia, and Department of Physics, University of Ljubljana, 1000 Ljubljana, Slovenia
[46] Fysikum, Stockholm University, Box 6730, 113 85 Stockholm, Sweden
[47] Dipartimento di Fisica Sperimentale, Università di Torino and INFN, Via P. Giuria 1, 10125 Turin, Italy
[48] Dipartimento di Fisica, Università di Trieste and INFN, Via A. Valerio 2, 34127 Trieste, Italy and Istituto di Fisica, Università di Udine, 33100 Udine, Italy
[49] Univ. Federal do Rio de Janeiro, C.P. 68528 Cidade Univ., Ilha do Fundão 21945-970 Rio de Janeiro, Brazil
[50] Department of Radiation Sciences, University of Uppsala, P.O. Box 535, 751 21 Uppsala, Sweden
[51] IFIC, Valencia-CSIC, and D.F.A.M.N., U. de Valencia, Avda. Dr. Moliner 50, 46100 Burjassot (Valencia), Spain
[52] Institut für Hochenergiephysik, Österr. Akad. d. Wissensch., Nikolsdorfergasse 18, 1050 Vienna, Austria
[53] Inst. Nuclear Studies and University of Warsaw, Ul. Hoza 69, 00681 Warsaw, Poland
[54] Fachbereich Physik, University of Wuppertal, Postfach 100 127, 42097 Wuppertal, Germany

Received: 29 February 2000 / Revised version: 9 October 2000 /
Published online 27 November 2000 –

Abstract. Inclusive distributions of charged particles in hadronic W decays are experimentally investigated using the statistics collected by the DELPHI experiment at LEP during 1997, 1998 and 1999, at centre-of-mass energies from 183 to around 200 GeV. The possible effects of interconnection between the hadronic decays of two Ws are not observed. Measurements of the average multiplicity for charged and identified particles in $q\bar{q}$ and WW events at centre-of-mass energies from 130 to 200 GeV and in W decays are presented. The results on the average multiplicity of identified particles and on the position ξ^* of the maximum of the $\xi_p = -\log(\frac{2p}{\sqrt{s}})$ distribution are compared with predictions of JETSET and MLLA calculations.

1 Introduction

The study of the production properties of charged and identified hadrons (π^+, K^+, K^0, p and Λ)[1] in $q\bar{q}$ events at LEP 2 allows QCD based models to be tested through the comparison with LEP 1 data, in particular the validity of high-energy extrapolations of Monte Carlo models tuned at the Z^0.

In the case of WW events in which both W bosons decay hadronically, these kind of studies, besides providing checks for QCD-inspired models, are expected to give insights into possible correlations and/or final state interactions between the decay products of the two W bosons.

Hadron production in e^+e^- and QCD

The way quarks and gluons transform into hadrons is complex and can not be completely described by QCD. In the Monte Carlo simulations (as in [1]), the hadronisation of a $q\bar{q}$ pair is split into 3 phases. In a first phase, gluon emission and parton branching of the original $q\bar{q}$ pair take place. It is believed that this phase can be described by perturbative QCD (most of the calculations have been performed in leading logarithmic approximation LLA). In a second phase, at a certain virtuality cut-off scale Q_0, where $\alpha_s(Q_0)$ is still small, quarks and gluons produced in the first phase are clustered in colour singlets and transform into mesons and baryons. Only phenomenological models, which need to be tuned to the data, are available to describe this stage of fragmentation; the models most frequently used in e^+e^- annihilations are based on string and cluster fragmentation. In the third phase, the unstable states decay into hadrons which can be observed and identified in the detector. These models account correctly for most of the features of the $q\bar{q}$ events such as, for instance, the average multiplicity and inclusive momentum spectra.

A different and purely analytical approach (see e.g. [2] and references therein) giving quantitative predictions of hadronic spectra are QCD calculations using the so-called Modified Leading Logarithmic Approximation (MLLA) under the assumption of Local Parton Hadron Duality (LPHD) [3,4]. In this picture multi-hadron production is described by a parton cascade, and the virtuality cut-off Q_0 is lowered to values of the order of 100 MeV, comparable to the hadron masses; it is assumed that the results obtained for partons are proportional to the corresponding quantities for hadrons.

[1] Unless otherwise stated antiparticles are included as well

The MLLA/LPHD predictions involve three parameters: an effective scale parameter $\Lambda_{\rm eff}$, a virtuality cut-off Q_0 in the evolution of the parton cascade and an overall normalisation factor $K_{\rm LPHD}$. The momentum spectra of hadrons can be calculated as functions of the variable $\xi_p = -\ln(\frac{2p}{\sqrt{s}})$, with p being the particle's momentum and $\sqrt{s}$ the centre-of-mass energy:

$$\frac{dn}{d\xi_p} = K_{\rm LPHD} \cdot f(\xi_p, X, \lambda) \tag{1}$$

with

$$X = \log\frac{\sqrt{s}}{Q_0}\ ;\ \lambda = \log\frac{Q_0}{\Lambda_{\rm eff}}\,. \tag{2}$$

Due to uncertainties from higher order corrections Λ_{eff} cannot be identified with $\Lambda_{\overline{MS}}$. In (1), n is the average multiplicity per bin of ξ_p, and the function f has the form of a "hump-backed plateau". It can be approximated by a distorted Gaussian [5,6]

$$DG(\xi; N, \overline{\xi}, \sigma, s_k, k) = \frac{N}{\sigma\sqrt{2\pi}} \exp\left(\frac{1}{8}k + \frac{1}{2}s_k\delta - \frac{1}{4}(2+k)\delta^2 + \frac{1}{6}s_k\delta^3 + \frac{1}{24}k\delta^4\right)\ , \tag{3}$$

where $\delta = (\xi - \overline{\xi})/\sigma$, $\bar{\xi}$ is the mean of the distribution, σ is the square root of its variance, s_k its skewness and k its kurtosis. For an ordinary Gaussian these last two parameters vanish. The mean, $\overline{\xi}$, coincides with the peak of the distribution, ξ^*, only up to next-to-leading order in α_s.

To check the validity of the MLLA/LPHD approach, one can study the evolution of the position of the maximum, ξ^*, as a function of $\sqrt{s}$. In the context of MLLA/LPHD the dependence of ξ^* on the centre-of-mass energy can be expressed as [2,5]:

$$\xi^* = Y\left(\frac{1}{2} + \sqrt{C/Y} - C/Y\right) + F_h(\lambda), \tag{4}$$

where

$$Y = log\frac{\sqrt{s}/2}{\Lambda_{\rm eff}}\ ,$$
$$C = \left(\frac{11N_c/3 + 2n_f/(3N_c^2)}{4N_c}\right)^2 \cdot \left(\frac{N_c}{11N_c/3 - 2n_f/3}\right), \tag{5}$$

with N_c being the number of colours and n_f the number of active quark flavours in the fragmentation process. The function $F_h(\lambda)$ depends on the hadron type through $\lambda = \log(Q_0/\Lambda_{eff})$ [2], and it can be approximated as $F_h(\lambda) = -1.46\lambda + 0.207\lambda^2$ with an error of ± 0.06.

Interference and final state interactions in W decays

The possible presence of interference due to colour reconnection and Bose-Einstein correlations (see for example [7–12] and [13,14] for reviews) in hadronic decays of WW pairs may provide information on hadron formation at a time scale smaller than 1 fm/c. At the same time it can induce a systematic uncertainty on the W mass measurement in the 4-jet mode [13] comparable with the expected accuracy of the measurement at LEP 2.

Interconnection can happen due to the fact that the lifetime of the W ($\tau_W \simeq \hbar/\Gamma_W \simeq 0.1$ fm/c) is an order of magnitude smaller than the typical hadronisation times. The interconnection between the products of the hadronic decays of different Ws in WW pair events can occur at several stages: (1) from colour rearrangement between the quarks coming from the primary branching, (2) due to gluon exchanges during the parton cascade, (3) in the mixing of identical pions or kaons due to Bose-Einstein correlations. The first two are QCD effects. They can mix the two colour singlets and produce hadrons which cannot be uniquely assigned to either W. The perturbative effects are colour suppressed and the possible shift is expected to be only about 5 MeV in the W mass [7].

Non-perturbative effects need model calculations. Several models have been proposed (for reviews see for example [13] and [15]) and have already been included in the widely used event generators PYTHIA [1], ARIADNE [16] and HERWIG [17]. In these models the final state quarks after the parton shower can be rearranged to form colour singlets with probabilities which in some cases are free parameters. The shift on the W mass in these models is typically smaller than 50 MeV [18], but other observables are affected by colour rearrangement. Generally these models suggest a small effect on the total charged particle multiplicity, of the order of -1% to -2% [15,19,14]. Dedicated detailed simulations of the response of the DELPHI detector to such models showed that this effect is substantially unaffected by the event selection criteria and by the detector performance. For identified heavy particles, such as K^+ and p, the effects due to colour reconnection are expected to be stronger [20], but the experimental verification is complicated by losses in statistics. The same applies to the particle spectrum at low momentum [15]. Bose-Einstein Correlations could also slightly change the multiplicity for ($4q$) events in some models [12,21].

The WW events allow a comparison of the characteristics of the W hadronic decays when both Ws decay in hadronic modes (referred to here as the ($4q$) mode) with the case in which only one W decays hadronically (($2q$) mode). These characteristics should be the same in the absence of interference between the hadronic decay products from different W bosons.

Previous experimental results based on the statistics collected by LEP experiments during 1997 (see [22–24] for reviews) did not indicate at that level of statistics the presence of interconnection or correlation effects.

This paper presents measurements of:

- the charged particle multiplicities for the $q\bar{q}$ events in the data sample collected by the DELPHI experiment at LEP during 1997, 1998 and 1999, at the centre-of-mass energies from 183, 189 and from 192 to 200 GeV respectively;

– the charged particle multiplicity and inclusive distributions for WW events at 183 and 189 GeV (multiplicity values at 189 GeV are expected to be slightly higher than that at 183 GeV due to increased phase space. However this effect is below the precision obtainable with the present data samples);
– The average multiplicities for identified charged and neutral particles (π^+, K^+, K^0, p and Λ), and the position ξ^* of the maximum of the ξ_p distribution for identified particles in $q\bar{q}$ events from 130 GeV to 189 GeV and in WW events at 189 GeV.

2 Data sample and event preselection at 183 and 189 GeV

Data corresponding to total luminosities of 157.7 pb^{-1} (54.1 pb^{-1}) at centre-of-mass energies around 189 (183) GeV, and data taken in 1999 corresponding to total luminosities of 25.8 pb^{-1}, 77.4 pb^{-1} and 83.8 pb^{-1} at centre-of-mass energies around 192 GeV, 196 GeV and 200 GeV respectively were analysed. A description of the DELPHI detector can be found in [25]; its performance is discussed in [26].

A preselection of hadronic events was made, requiring at least 6 charged particles and a total transverse energy of all the particles above 20% of the centre-of-mass energy $\sqrt{s}$. In the calculation of the energies E, all charged particles were assumed to have the pion mass. Charged particles were required to have momentum p above 100 MeV/c and below 1.5 times the beam energy, a relative error on the momentum measurement $\Delta p/p < 1$, angle θ with respect to the beam direction between 20° and 160°, and a distance of closest approach to the interaction point less than 4 cm in the plane perpendicular to the beam axis (2 cm in the analyses of identified charged particles) and less than $4/\sin\theta$ cm along the beam axis (2 cm in the analyses of identified charged particles).

After the event selection charged particles were also required to have a track length of at least 30 cm, and in the charged identified particles analysis a momentum $p > 200$ MeV/c.

The influence of the detector on the analysis was studied with the full DELPHI simulation program, DELSIM [26]; events were generated with PYTHIA 5.7, using the JETSET fragmentation with Parton Shower (PS) [1] with parameters tuned to fit LEP 1 data from DELPHI [27]. The initial state for the WW 1999 sample was generated using EXCALIBUR version 1.08 [28]. The particles were followed through the detailed geometry of DELPHI with simulated digitizations in each detector. These data were processed with the same reconstruction and analysis programs as the real data.

To check the ability of the simulation to model the efficiency for the reconstruction of charged particles, the samples collected at the Z^0 pole during 1998 and 1997 were used. From these samples, by integrating the distribution of $\xi_E = -\ln(\frac{2E}{\sqrt{s}})$, where E is the energy of the particle, corrected bin by bin using the simulation, the average charged particle multiplicities at the Z^0 were measured. The values were found to be $20.93 \pm 0.03(stat)$ and $20.60 \pm 0.03(stat)$ respectively, in satisfactory agreement with the world average of 21.00 ± 0.13 [29]. The ratios of the world average value to the measured multiplicities at the Z^0, respectively 1.0033 ± 0.0064 and 1.0194 ± 0.0065 from the Z^0 data in 1998 and 1997, were used to correct the measured multiplicities at high energies in the respective years.

The cross-section for $e^+e^- \to q\bar{q}(\gamma)$ above the Z^0 peak is dominated by radiative $q\bar{q}\gamma$ events; the initial state radiated photons (ISR photons) are generally aligned along the beam direction and not detected. In order to compute the hadronic centre-of-mass energy, $\sqrt{s'}$, the procedure described in [30] was used. The procedure clusters the particles into jets using the DURHAM algorithm [31], excluding candidate ISR photons and using a $y_{cut} = 0.002$. The reconstructed jets and additional ISR photons are then fitted with a three constraint fit (energy and transverse momentum, leaving free the z component of the missing momentum). The hadronic centre-of-mass energy, $\sqrt{s'}$, is the invariant mass of the jets using the fitted jet energies and directions.

3 Analysis of charged particles in $q\bar{q}$ events

3.1 Centre-of-mass energies of 183 and 189 GeV

Events with $\sqrt{s'}/\sqrt{s}$ above 0.9 were used to compute the multiplicities. A total of 3444 (1297) hadronic events were selected from the data at 189 (183) GeV, by requiring that the multiplicity for charged particles was larger than 9, that the total transverse energy of the charged particles exceeded $0.2\sqrt{s}$, and that the narrow jet broadening [32] was smaller than 0.065. From the simulation it was calculated that the expected background coming from WW and Z^0Z^0 decays was 432+52 (127+21) events. The contamination from double radiative returns to the Z^0, within 10 GeV of the nominal Z^0 mass, was estimated by simulation to be below 5%. Other contaminations (from Z^0ee, Weν, $\gamma\gamma$ interactions and Bhabhas) are below 2% in total.

The average multiplicity of charged particles with $p > 0.1$ GeV/c measured in the selected events at 189 GeV (183 GeV), after subtraction of the WW and Z^0Z^0 backgrounds estimated by simulation, was $24.58 \pm 0.16(stat)$ ($23.96 \pm 0.23(stat)$), to be compared to $24.52 \pm 0.05(stat)$ ($24.30 \pm 0.07(stat)$) in the $q\bar{q}$ PS simulation including detector effects. The dispersion (square root of the variance) of the multiplicity distribution in the data was $7.57 \pm 0.11(stat)$ ($7.00 \pm 0.16(stat)$), to be compared to the dispersion from the $q\bar{q}$ PS simulation of 7.24 ± 0.03 ($7.20 \pm 0.05(stat)$).

Detector effects and selection biases were corrected for using a $q\bar{q}$ simulation from PYTHIA with the JETSET fragmentation tuned by DELPHI without inital state radiation. The corrected average charge multiplicity was found to be $< n >= 27.37 \pm 0.18(stat)$ ($< n >= 26.56 \pm 0.26(stat)$), and the dispersion was found to be $D = 8.77 \pm 0.13(stat)$ ($D = 8.08 \pm 0.19(stat)$).

The average multiplicity was computed by integrating the ξ_E distribution, since the detection efficiency depends mostly on the momentum of the particle, after correcting for detector effects bin by bin using the simulation. The ξ_E distribution was integrated up to a value of 6.3, and the extrapolation to the region above this cut was based on the simulation at the generator level.

After multiplying by the Z^0 corrections factors from Sect. 2, the following values were obtained:

$$\langle n \rangle_{189\,\mathrm{GeV}} = 27.47 \pm 0.18(stat) \pm 0.30(syst) \quad (6)$$
$$D_{189\,\mathrm{GeV}} = 8.77 \pm 0.13(stat) \pm 0.11(syst) \quad (7)$$
$$\langle n \rangle_{183\,\mathrm{GeV}} = 27.05 \pm 0.27(stat) \pm 0.32(syst) \quad (8)$$
$$D_{183\,\mathrm{GeV}} = 8.08 \pm 0.19(stat) \pm 0.14(syst)\,. \quad (9)$$

These values include the products of the decays of particles with lifetime $\tau < 10^{-9}$ s.

The systematic errors were obtained by adding in quadrature:

1. the propagated uncertainty of the average values in the Z^0 correction factors, ± 0.18 (± 0.17) for the multiplicity.
2. the effect of the cuts for the reduction of the background. The value of the cut on the narrow jet broadening was varied from 0.045 to 0.085 in steps of 0.010, in order to estimate the systematic error associated with the procedure of removing the contribution from WW events. The new values for the average charged particle multiplicity and the dispersion were stable within these variations, and half of the difference between the extreme values, 0.07 and 0.07 (0.06 and 0.12) respectively, were added in quadrature to the systematic error. The effect of the uncertainty on the WW cross-section was found to be negligible.
3. the uncertainty on the modelling of the detector response in the forward region. The analysis was repeated by varying the polar angle acceptance of charged particles from 10-170 degrees to 40-140 degrees, both in the high energy samples and in the computation of the Z^0 correction factors. The spread of the different values obtained for the multiplicities and for the dispersions were found to be respectively 0.18 and 0.08 (0.23 and 0.03). The effect of the variation of other track selection criteria was found to be negligible, and the same applies to the higher centre-of-mass energies.
4. the systematic errors due to the statistics of the simulated samples, 0.04 (0.06) for the multiplicity and 0.04 (0.06) for the dispersion.
5. the uncertainty on the calculation of the efficiency correction factors in the multiplicity. The values of the multiplicities, before applying the Z^0 correction factors, were also estimated:
   - from the observed multiplicity distribution as 27.37 (26.56);
   - from the integral of the rapidity distribution (with respect to the thrust axis), $y_T = \frac{1}{2} \ln \frac{E+p_{||}}{E-p_{||}}$ ($p_{||}$ is the absolute value of the momentum component on the thrust axis) as 27.43 (26.59).

   Half of the differences between the maximum and the minimum values of the multiplicity calculated from the multiplicity distribution and from the integration of the y_T and ξ_E distributions, 0.03 in both cases, were added in quadrature to the systematic error.
6. Half of the extrapolated multiplicity in the high-ξ_E region, 0.14 (0.12).

As a cross-check, a simulated sample based on HERWIG plus DELSIM was also used to unfold the data; the results were consistent with those based on PYTHIA plus DELSIM within the statistical error associated to the size of the Monte Carlo sample.

3.2 Centre-of-mass energies of 192 to 200 GeV

To check the ability of the simulation to model the efficiency for the reconstruction of charged particles, the sample collected at the Z^0 calibration runs of 1999 was used, following the procedure described in Sect. 2. The average charged particle multiplicity at the Z^0 was measured to be $20.82 \pm 0.03(stat)$, in satisfactory agreement with the world average. The ratio of the world average value to the measured multiplicity at the Z^0, 1.0084 ± 0.0064, was used to correct the measured multiplicities at centre-of-mass energies of 192 to 200 GeV.

For each of the energies a separate analysis was performed following the procedure described in the previous subsection.

The number of events selected, the number of expected signal and background events, estimated with Monte Carlo simulation, and the measured multiplicities and dispersions are listed in Table 1 for the centre-of-mass energies of 192 to 200 GeV. The systematic errors were estimated as in 3.1; a breakdown is shown in the table (the numbering of the sources of systematic error corresponds to the one in the previous subsection).

These results were then combined at an average centre-of-mass energy of 200 GeV, according to the following procedure. First each result was rescaled to a centre-of-mass energy of 200 GeV, calculating the scaling factors from the simulation. Then a weighted average was computed using the statistical error as a weight. The systematic error is taken as the weighted average of the systematic errors, increased (in quadrature) by the difference between the values obtained when rescaling and when not rescaling to 200 GeV. This gives:

$$\langle n \rangle_{200\,\mathrm{GeV}} = 27.58 \pm 0.19(stat) \pm 0.45(syst) \quad (10)$$
$$D_{200\,\mathrm{GeV}} = 8.64 \pm 0.13(stat) \pm 0.20(syst)\,. \quad (11)$$

As a cross-check, a simulated sample based on HERWIG plus DELSIM was also used to unfold the data; the results were consistent with those based on PYTHIA plus DELSIM within the statistical error associated to the size of the Monte Carlo sample.

Table 1. Number of events selected, number of events expected for the signal ($q\bar{q}\gamma$) and for the background (WW and ZZ), estimated from simulation, and the measured multiplicities and dispersions for the three different energies

	192 GeV	196 GeV	200 GeV
Selected events	526	1542	1580
Expected $q\bar{q}$ events	431	1253	1277
Expected background events	84	267	307
$\langle n \rangle$	27.19	27.42	27.52
statistical error	0.47	0.28	0.29
systematic error	0.51	0.37	0.44
(syst. 1)	0.17	0.17	0.17
(syst. 2)	0.35	0.08	0.18
(syst. 3)	0.29	0.27	0.30
(syst. 4)	0.06	0.05	0.08
(syst. 5)	0.03	0.01	0.01
(syst. 6)	0.15	0.17	0.19
D	8.57	8.52	8.69
statistical error	0.34	0.20	0.21
systematic error	0.32	0.14	0.19
(syst. 2)	0.30	0.12	0.16
(syst. 3)	0.09	0.06	0.05
(syst. 4)	0.06	0.05	0.09

4 Classification of the WW events and charged multiplicity measurement

About 4/9 of the WW events are WW $\to q_1\bar{q}_2q_3\bar{q}_4$ events. At threshold, their topology is that of two pairs of back-to-back jets, with no missing energy; the constrained invariant mass of two jet-jet systems is close to the W mass. Even at 183 and 189 GeV these characteristics allow a clean selection.

Another 4/9 of the WW events are WW $\to q_1\bar{q}_2\,\ell\bar{\nu}$ events. At threshold, their topology is 2-jets back-to-back, with a lepton and missing energy opposite to it; the constrained invariant mass of the jet-jet system and of the lepton-missing energy system equals the W mass.

4.1 Fully hadronic channel (WW $\to q_1\bar{q}_2q_3\bar{q}_4$)

Events with both Ws decaying into $q\bar{q}$ are characterised by high multiplicity, large visible energy, and tendency of the particles to be grouped in 4 jets. The background is dominated by $q\bar{q}(\gamma)$ events.

The events were pre-selected by requiring at least 12 charged particles (with $p > 100$ MeV/c), with a total transverse energy (charged plus neutral) above 20% of the centre-of-mass energy. To remove the radiative hadronic events, the effective hadronic centre-of-mass energy $\sqrt{s'}$, computed as described in Sect. 2, was required to be above 110 GeV.

The particles in the event were then clustered to 4 jets using the LUCLUS algorithm [1], and the events were kept if all jets had multiplicity (charged plus neutral) larger than 3. It was also required that the separation between the jets ($d_{\rm join}$ value) be larger than 6 GeV/c. The combination of these two cuts removed most of the remaining semi-leptonic WW decays and the 2-jet and 3-jet events of the $q\bar{q}\gamma$ background.

A five constraint fit was applied, imposing energy and momentum conservation and the equality of two di-jet masses. Of the three fits obtained by permutation of the jets, the one with the smallest χ^2 was selected. Events were accepted only if

$$D_{sel} = \frac{E_{min}\theta_{min}}{E_{max}(E_{max} - E_{min})} > 0.004\,\text{rad GeV}^{-1}$$

where E_{min} and E_{max} are respectively the smallest and the largest fitted jet energy, and θ_{min} is the smallest angle between the fitted jet directions. The details of the selection variable D_{sel} can be found in [33]. The purity and the efficiency of the selected data sample from the 189 (183) GeV data were estimated using simulation to be about 76% and 80% (75% and 80%) respectively. The data sample consists of 1256 (427) events, where 1255 (422) were expected from the simulation. The expected background was subtracted bin by bin from the observed distributions, which were then corrected bin by bin using scaling factors computed from the simulation generated using PYTHIA with the JETSET fragmentation tuned by DELPHI (EXCALIBUR plus JETSET for the 1999 data) without initial state radiation.

Finally, the average multiplicity of charged particles $\langle n^{(4q)} \rangle$ was estimated by integrating the ξ_E distribution up to a value of 6.3 (and estimated above this value with simulation) and multiplying by the Z^0 correction factors from Sect. 2. The following values were obtained:

$$\langle n^{(4q)} \rangle_{189\,\text{GeV}} = 39.12 \pm 0.33(stat) \pm 0.36(syst) \quad (12)$$

$$\langle n^{(4q)} \rangle_{183\,\text{GeV}} = 38.11 \pm 0.57(stat) \pm 0.44(syst)\,. \quad (13)$$

The systematic errors account for:

1. The propagated uncertainty of the average values in the Z^0 correction factors, ± 0.24 (± 0.24).
2. The spread of the measured values from the reference values by redoing the analysis varying the selection criteria, 0.05 (0.11).
3. Modelling of the detector in the forward region. The analysis was repeated by varying the polar angle acceptance of charged particles from 10-170 degrees to 40-140 degrees, both in the WW samples and in the computation of the Z^0 correction factors. The spreads of the different measured values were found to be 0.01 (0.08).
4. Limited statistics in the simulated sample 0.03 (0.05).
5. Variation of the $q\bar{q}\gamma$ cross-sections within 5%: 0.01 (0.01).
6. Calculation of the correction factors. The value of $\langle n^{(4q)} \rangle$, before applying the Z^0 correction factors, was also estimated:

- from the observed multiplicity distribution as 38.96 (37.39);
- from the integral of the rapidity distribution (with respect to the thrust axis) as 39.16 (36.97).
- from the integral of the p_T distribution (with respect to the thrust axis) as 38.95 (37.42).

Half of the difference between the maximum and the minimum value, 0.11 (0.23), was added in quadrature to the systematic error.

7. Uncertainty on the modelling of the 4-jets $q\bar{q}$ background, 0.05 (0.14). The uncertainty on the modelling of this background is the sum in quadrature of two contributions:
   - Uncertainty on the modelling of the 4-jet rate. The agreement between data and simulation was studied in a sample of 4-jet events at the Z^0, selected with the DURHAM algorithm for y_{cut} ranging from 0.003 to 0.005. The rate of 4-jet events in the simulated sample was found to reproduce the data within 10%. The correction due to background subtraction was correspondingly varied by 10%, which gives an uncertainty of 0.00 (0.01).
   - Uncertainty on the multiplicity in 4-jet events. The average multiplicity in 4-jet events selected at the Z^0 data in 1998 (1997), with the DURHAM algorithm for a value of $y_{cut} = 0.005$, is larger by $0.9\%\pm0.3\%(stat)$ ($2.0\%\pm0.5\%(stat)$) than the corresponding value in the simulation. A shift by 0.9% (2.0%) in the multiplicity for 4-jet events induces a shift of 0.05 (0.14) on the value in (12) (13).
8. Half of the extrapolated multiplicity in the high-ξ_E region, 0.23 (0.20).

The presence of interference between the jets coming from the different Ws could create subtle effects, such as to make the application of the fit imposing equal masses inadequate. For this reason a different four constraint fit was performed, leaving the di-jet masses free and imposing energy-momentum conservation. Of the three possible combinations of the four jets into WW pairs, the one with minimum mass difference was selected. No χ^2 cut was imposed in this case. The average multiplicity obtained was again fully consistent (within the statistical error) with the one measured in the standard analysis.

A simulated sample based on HERWIG plus DELSIM was also used to unfold the data; the results were consistent with those based on PYTHIA plus DELSIM within the statistical error associated to the size of the Monte Carlo sample.

The distribution of the observed charged particle multiplicity in ($4q$) is shown in Fig. 1c(1a).

The value of the corrected multiplicity in the low momentum range 0.1 to 1. GeV/c, where the interconnection effects are expected to be most important, was found to be 14.47 ± 0.20 (13.67 ± 0.34), where the errors are statistical only.

After correcting for detector effects, the dispersion was found to be:

$$D^{(4q)}_{189\,\mathrm{GeV}} = 8.72 \pm 0.23(stat) \pm 0.11(syst) \qquad (14)$$

$$D^{(4q)}_{183\,\mathrm{GeV}} = 8.53 \pm 0.39(stat) \pm 0.16(syst)\,. \qquad (15)$$

In the systematic error:

1. 0.10 (0.15) accounts for the spreads of the measured values from the reference value when varying the event selection criteria;
2. 0.03 (0.01) is due to the modelling of the detector in the forward region. The dispersions were also measured using only charged particles with polar angle between 40 and 140 degrees and the differences with respect to the reference value were considered in the systematic error;
3. 0.03 (0.05) from the limited simulation statistics.

4.2 Mixed hadronic and leptonic final states (WW$\rightarrow \mathrm{q_1\bar{q}_2}l\nu$)

Events in which one W decays into lepton plus neutrino and the other one into quark and antiquark are characterised by two hadronic jets, one energetic isolated charged lepton, and missing momentum resulting from the neutrino. The main backgrounds to these events are radiative $q\bar{q}$ production and four-fermion final states containing two quarks and two oppositely charged leptons of the same flavour.

Events were selected by requiring seven or more charged particles, with a total energy (charged plus neutral) above $0.2\sqrt{s}$ and a missing momentum larger than $0.1\sqrt{s}$. Events in the $q\bar{q}\gamma$ final state with ISR photons at small polar angles, which would be lost inside the beam pipe, were suppressed by requiring the polar angle of the missing momentum vector to satisfy $|\cos\theta_{miss}| < 0.94$.

Including the missing momentum as an additional massless neutral particle (the candidate neutrino), the particles in the event were clustered to 4 jets using the DURHAM algorithm. The jet for which the fractional jet energy carried by the highest momentum charged particle was greatest was considered as the "lepton jet". The most energetic charged particle in the lepton jet was taken as the lepton candidate, and the event was rejected if its momentum was smaller than 10 GeV/c. The neutrino was taken to correspond to the missing momentum. The event was discarded if the invariant mass of the event (excluding the lepton candidates) was smaller than 20 GeV/c^2 or larger than 110 GeV/c^2.

At this point three alternative topologies were considered:

- Muon sample: if the lepton candidate was tagged as a muon and its isolation angle, with respect to other charged particles above 1 GeV/c, was above 10°, the event was accepted either if the lepton momentum was greater than 20 GeV/c, or if it was greater than 10 GeV/c and the value of the $y^{cut}_{3\rightarrow4}$ parameter required by the DURHAM algorithm to force the event from a 3-jet to a 4-jet configuration was greater than 0.003.
- Electron sample: if the lepton candidate had associated electromagnetic energy deposited in the calorimeters

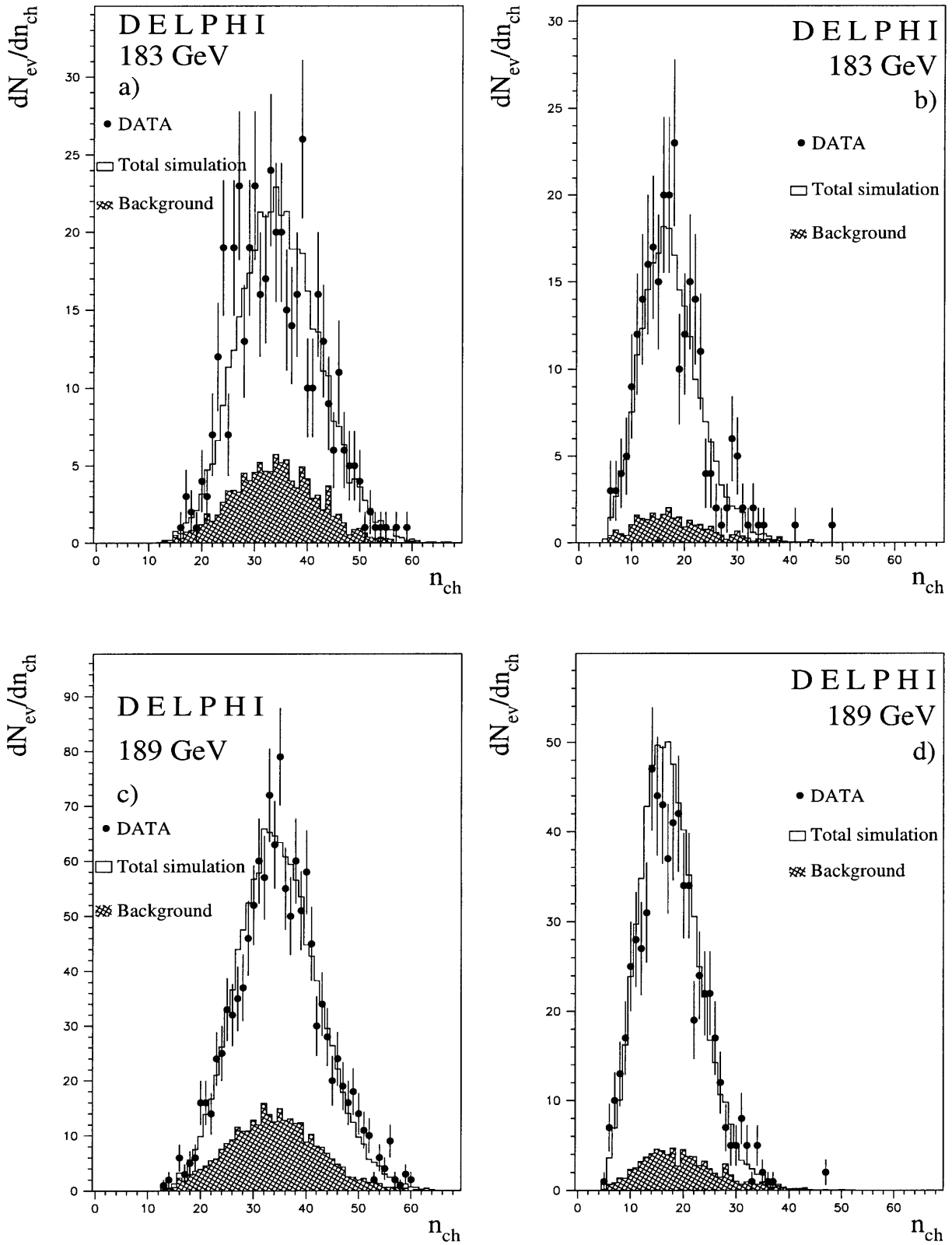

Fig. 1a–d. Charged particle multiplicity distributions for **a** the $(4q)$ events and **b** the $(2q)$ events at 183 GeV, for **c** the $(4q)$ events and **d** the $(2q)$ events at 189 GeV. The error bars in the data represent the statistical errors. The shaded areas represent the background contribution; the histograms are the sum of the expected signal and background

larger than 20 GeV, and an isolation angle (defined as above) greater than 10°, the event was accepted if the required value of $y_{3\to4}^{cut}$ was greater than 0.003.
– Inclusive sample: the events were also accepted if the momentum of the lepton candidate was larger than 20 GeV/c and greater than half of its associated energy, the missing momentum was larger than $0.1\sqrt{s}$, the required value of $y_{3\to4}^{cut}$ was greater than 0.003, and no other charged particle above 1 GeV/c existed in the lepton jet.

The purity and the efficiency of the selected data sample from the 189 (183) GeV data were estimated using simulation to be about 89% and 54% (88% and 55%) respectively. The data sample consists of 633 (256) events, where 689 (235) were expected from the simulation. The expected background was subtracted bin by bin from the observed distributions, which were then corrected bin by bin using scaling factors computed from the simulation generated using PYTHIA with the JETSET fragmentation tuned by DELPHI (EXCALIBUR plus JETSET for the 1999 data) without initial state radiation.

By integrating the ξ_E distribution up to a value of 6.3 (and estimated above this value from simulation at generator level), and multiplying by the Z^0 correction factors from Sect. 2, the following values were obtained for the charged multiplicity for one W decaying hadronically in a WW event with mixed hadronic and leptonic final states:

$$\langle n^{(2q)}\rangle_{189\,\mathrm{GeV}} = 19.49 \pm 0.31(stat) \pm 0.27(syst) \quad (16)$$

$$\langle n^{(2q)}\rangle_{183\,\mathrm{GeV}} = 19.78 \pm 0.49(stat) \pm 0.43(syst)\,. \quad (17)$$

In the systematic error:

1. 0.12 (0.12) accounts for the propagated uncertainty of the average values in the Z^0 correction factors;
2. 0.16 (0.16) accounts for the spreads from the reference values when changing the event selection criteria;
3. 0.05 (0.02) accounts for modelling of the detector in the forward region. The analysis was repeated by varying the polar angle acceptance of charged particles from 10-170 degrees to 40-140 degrees, both in the WW samples and in the computation of the Z^0 correction factors. The spreads of the different measured values were found to be 0.05 (0.02);
4. 0.03 (0.05) accounts for limited statistics in the simulated samples;
5. the variation of the $q\bar{q}(\gamma)$ cross-sections within 5%, gives a negligible contribution to the systematic error;
6. 0.12 (0.36) accounts for the uncertainty on the correction factors. The value of $\langle n^{(2q)}\rangle$, before applying the Z^0 correction factors, was also estimated:
   – from the observed multiplicity distribution as 19.53 (19.60);
   – from the integral of the rapidity distribution (with respect to the thrust axis) as 19.30 (18.88).
   – from the integral of the p_T distribution (with respect to the thrust axis) as 19.39 (19.36).

   Half of the difference between the maximum and the minimum value, 0.12 (0.36), was included in the systematic error.
7. Half of the extrapolated multiplicity in the high-ξ_E region, 0.12 (0.10).

A simulated sample based on HERWIG plus DELSIM was also used to unfold the data; the results were consistent with those based on PYTHIA plus DELSIM within the statistical error associated to the size of the Monte Carlo sample.

The distribution of the observed charged particle multiplicity in $(2q)$ is shown in Fig. 1d(1b).

The value of the corrected multiplicity in the low momentum range 0.1 to 1. GeV/c was found to be 7.29±0.19 (7.15±0.28) (where the errors are statistical only).

After correcting for detector effects, the dispersions were found to be:

$$D_{189\,\mathrm{GeV}}^{(2q)} = 6.49 \pm 0.21(stat) \pm 0.43(syst) \quad (18)$$

$$D_{183\,\mathrm{GeV}}^{(2q)} = 6.51 \pm 0.33(stat) \pm 0.25(syst)\,. \quad (19)$$

In the systematic error:

1. 0.14 (0.08) accounts for the variation of the cuts;
2. 0.41 (0.23) accounts for the modelling of the detector in the forward region. The dispersions were also measured using only charged particles with polar angle between 40 and 140 degrees and the differences with respect to the reference value were considered in the systematic error;
3. 0.03 (0.05) is due to the limited simulation statistics.

5 Analysis of interconnection effects from charged particle multiplicity and inclusive distributions

Most models predict that, in case of colour reconnection, the ratio between the multiplicity in $(4q)$ events and twice the multiplicity in $(2q)$ events would be smaller than 1; the difference is expected to be at the percent level. It was measured:

$$\left(\frac{\langle n^{(4q)}\rangle}{2\langle n^{(2q)}\rangle}\right)_{189\,\mathrm{GeV}} = 1.004 \pm 0.018(stat) \pm 0.014(syst) \quad (20)$$

$$\left(\frac{\langle n^{(4q)}\rangle}{2\langle n^{(2q)}\rangle}\right)_{183\,\mathrm{GeV}} = 0.963 \pm 0.028(stat) \pm 0.015(syst)\,. \quad (21)$$

In the calculation of the systematic error on the ratio, the correlations between the sources of systematic error were taken into account. If the systematic errors are taken as uncorrelated, except for the errors on the Z^0 correction factors and the modelling of the detector in the forward region, for which full correlation is assumed, a compatible value of ±0.014 (±0.022) is obtained for the systematic error.

Using as weights the inverse of the sum in quadrature of the statistical and systematic errors, one obtains a weighted average of

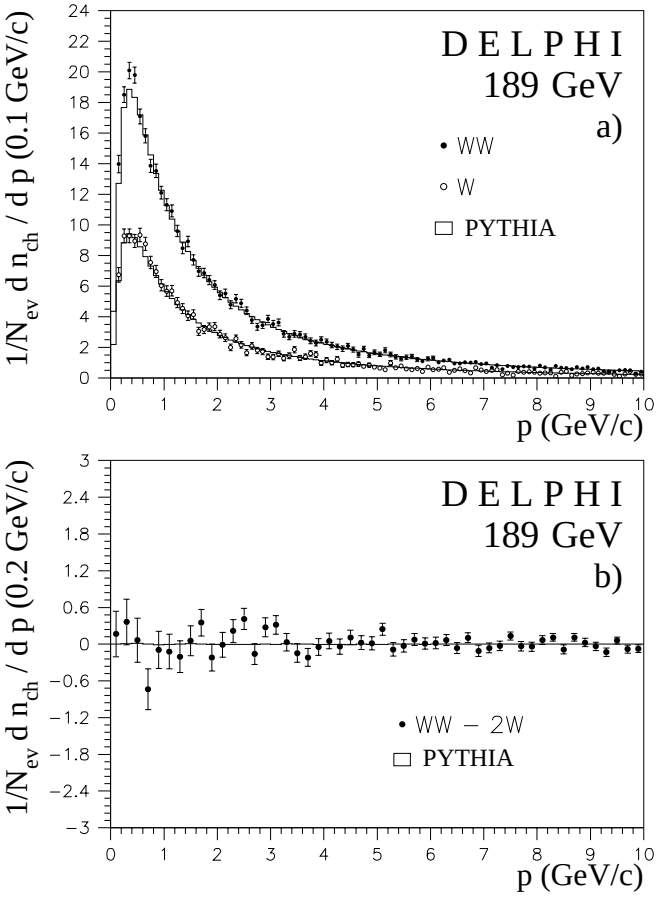

Fig. 2. **a** Corrected momentum distributions of charged particles for $(4q)$ events (closed circles) and $(2q)$ events (open circles), compared to simulation without colour reconnection, at 189 GeV. The error bars in the data represent the statistical errors. The difference between $(4q)$ and twice $(2q)$ is shown in **b**

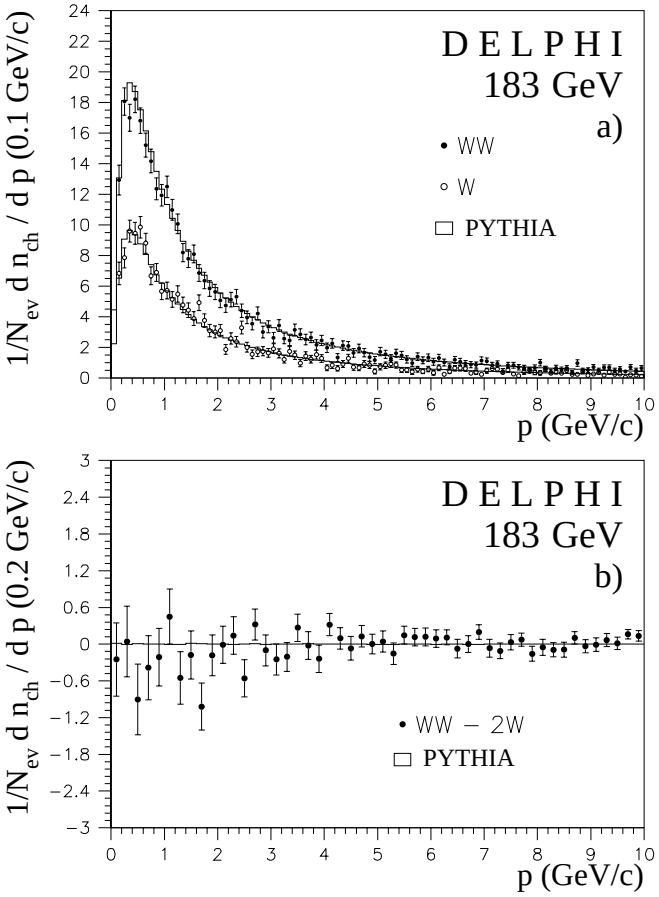

Fig. 3. **a** Corrected momentum distributions of charged particles for $(4q)$ events (closed circles) and $(2q)$ events (open circles), compared to simulation without colour reconnection, at 183 GeV. The difference between $(4q)$ and twice $(2q)$ is shown in **b**

$$\left(\frac{\langle n^{(4q)}\rangle}{2\langle n^{(2q)}\rangle}\right) = 0.990 \pm 0.015(stat) \pm 0.011(syst). \quad (22)$$

In the presence of interconnection, the deficit of multiplicity is expected to be concentrated in the region of low momentum. The corrected momentum distributions in the $(4q)$ and in the $(2q)$ cases are shown in Figs. 2 and 3 (Figs. 4 and 5 show the distributions in terms of the ξ_E variable). The systematic error in the momentum region between 0.1 and 1 GeV/c was explicitely recomputed. We measure:

$$\left.\frac{\langle n^{(4q)}\rangle}{2\langle n^{(2q)}\rangle}\right|^{0.1<p<1\,GeV/c}_{189\,\mathrm{GeV}} = 0.992 \pm 0.029(stat) \pm 0.016(syst) \quad (23)$$

$$\left.\frac{\langle n^{(4q)}\rangle}{2\langle n^{(2q)}\rangle}\right|^{0.1<p<1\,GeV/c}_{183\,\mathrm{GeV}} = 0.956 \pm 0.044(stat) \pm 0.022(syst)\,. \quad (24)$$

Using as weights the inverse of the sum in quadrature of the statistical and systematic errors, one obtains a weighted average of

$$\left.\frac{\langle n^{(4q)}\rangle}{2\langle n^{(2q)}\rangle}\right|^{0.1<p<1\,GeV/c} = 0.981 \pm 0.024(stat) \pm 0.013(syst). \quad (25)$$

Other inclusive distributions (rapidity and p_T for example) taking into account the orientation of particles could display a larger sensitivity with respect to interconnection effects. Special care should be taken, since the definition of the thrust axis could introduce a bias between $(2q)$ and $(4q)$ events. To estimate the effect of this bias, the following procedure was used. First the distributions of rapidity and p_T were computed as in the case of the momentum for the $(2q)$ and the $(4q)$. Then, a set of $(4q)$ -like events was constructed by mixing pairs of $(2q)$ events (constructed $(4q)$ sample). To construct this sample the hadronically decaying Ws in $(2q)$ events were boosted back to their rest frame. For each real $(4q)$ event, each W was then replaced by a W from a $(2q)$, boosted forward in such a way that the directions of the jet axis were the same.

If there would be no bias from the definition of the thrust axis (or if the correction for detector effects could correctly account for the bias), there would be no dif-

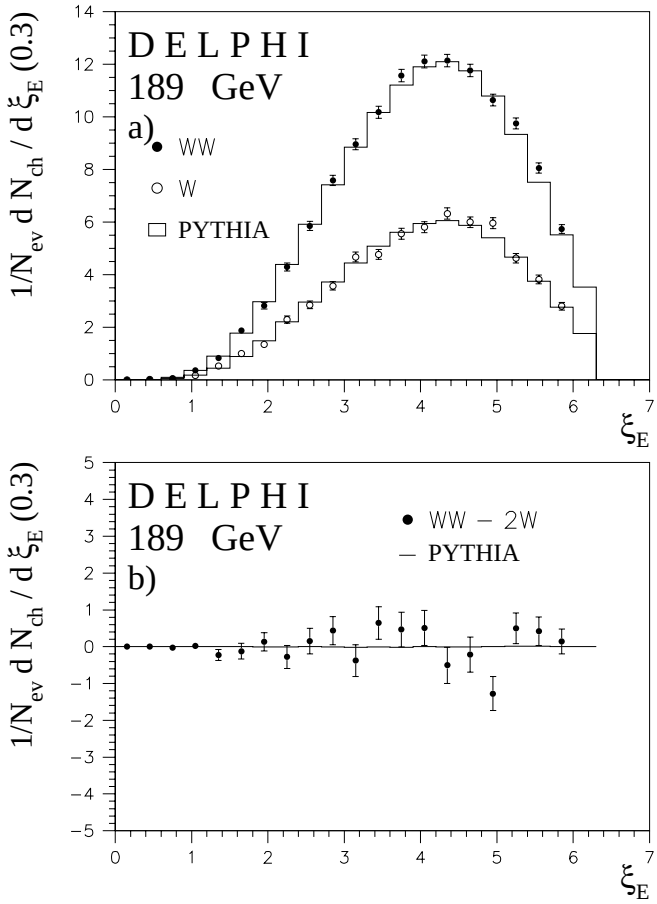

Fig. 4. **a** Corrected ξ_E distributions of charged particles for $(4q)$ events (closed circles) and $(2q)$ events (open circles), at 189 GeV, compared to simulation without colour reconnection. The error bars in the data represent the statistical errors. The difference between $(4q)$ and twice $(2q)$ is shown in **b**

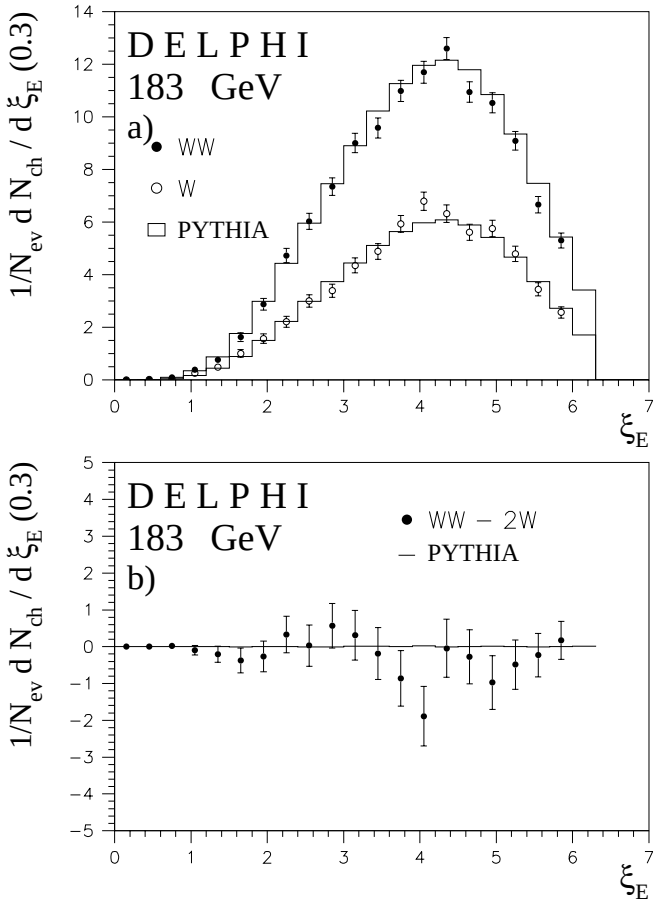

Fig. 5. **a** Corrected ξ_E distributions of charged particles for $(4q)$ events (closed circles) and $(2q)$ events (open circles), at 183 GeV, compared to simulation without colour reconnection. The error bars in the data represent the statistical errors. The difference between $(4q)$ and twice $(2q)$ is shown in **b**

ference between the y_T and p_T distributions in the constructed $(4q)$ sample and twice the $(2q)$ sample. This difference has thus been taken as an estimator of the systematic error from the bias, and added in quadrature to the $(4q)$ distribution, to twice the $(2q)$ distribution, and to their difference. The distributions of transverse momentum with respect to the thrust axis are shown in Figs. 6 and 7. It can be seen that the difference between the $(4q)$ distribution and twice the $(2q)$ at 183 GeV is concentrated in the low-p_T region; however, part of the difference is due to the fact that the $(2q)$ distribution at low p_T lies above the simulation. The rapidity distribution, instead, does not display any particular feature.

The dispersion in $(4q)$ events is consistent at both energies with $\sqrt{2}$ times the dispersion in $(2q)$ events (in the calculation of the systematic error on the ratio, the correlations between the sources of systematic error were taken into account):

$$\left(\frac{D^{(4q)}}{\sqrt{2}D^{(2q)}}\right)_{189\,\mathrm{GeV}} = 0.95 \pm 0.04(\mathrm{stat}) \pm 0.07(\mathrm{syst})$$

$$\left(\frac{D^{(4q)}}{\sqrt{2}D^{(2q)}}\right)_{183\,\mathrm{GeV}} = 0.93 \pm 0.06(\mathrm{stat}) \pm 0.04(\mathrm{syst})\,.$$

Using as weights the inverse of the sum in quadrature of the statistical and systematic errors, one obtains a weighted average of

$$\left(\frac{D^{(4q)}}{\sqrt{2}D^{(2q)}}\right) = 0.94 \pm 0.03(stat) \pm 0.03(syst). \qquad (26)$$

In conclusion, no depletion of the multiplicity was observed in fully hadronic WW events with respect to twice the semileptonic events, at this statistical precision; a possible depletion at the percent level can however not be excluded.

6 Identified particles from $e^+e^- \to \mathrm{q\bar{q}}$

This section describes the results obtained for π^+, K^+, K^0, p and Λ with data recorded by DELPHI at LEP 2.

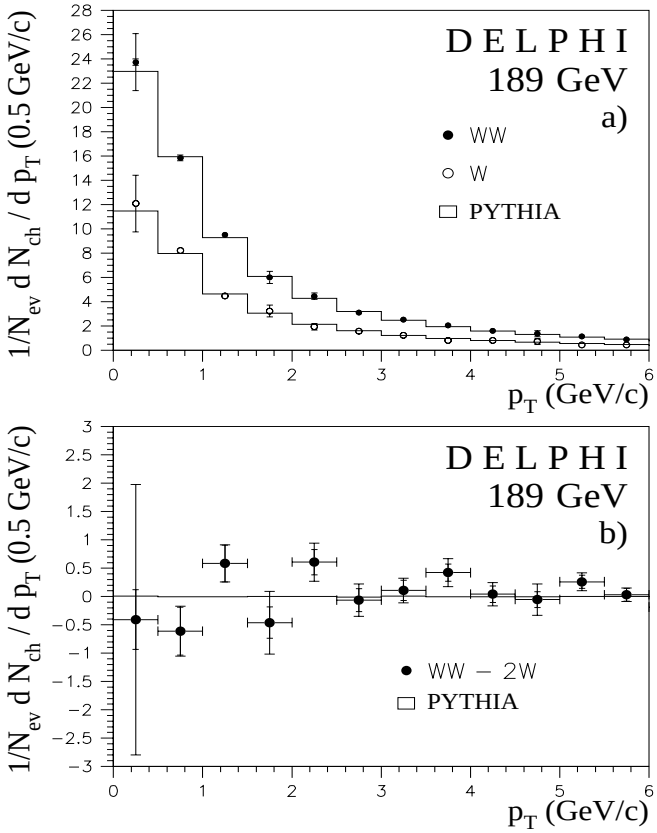

Fig. 6. **a** Corrected p_T distributions of charged particles for $(4q)$ events (closed circles) and $(2q)$ events (open circles), compared to simulation without colour reconnection, at 189 GeV. The internal error bars in the data represent the statistical error and the external error bars represent the sum in quadrature of the statistical and systematic errors. The difference between $(4q)$ and twice $(2q)$ is shown in **b**

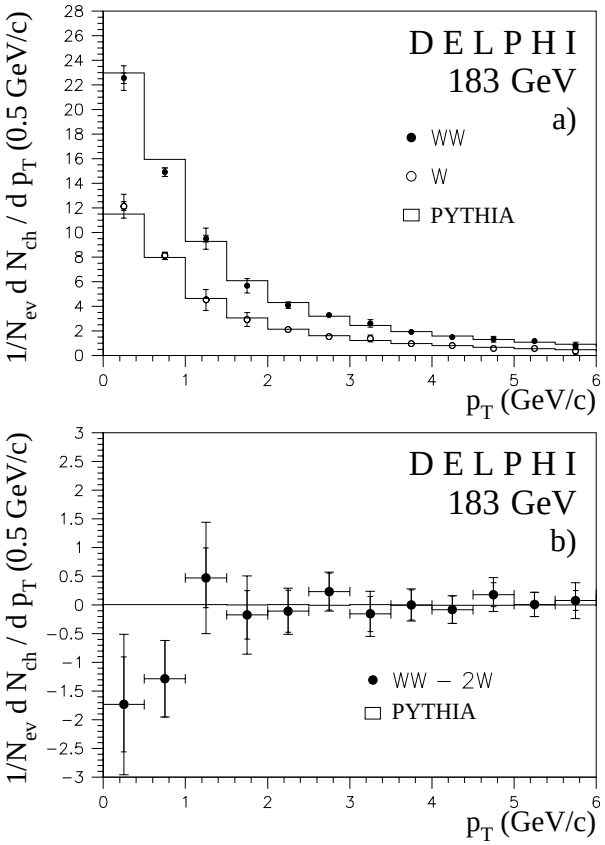

Fig. 7. **a** Corrected p_T distributions of charged particles for $(4q)$ events (closed circles) and $(2q)$ events (open circles), compared to simulation without colour reconnection, at 183 GeV. The internal error bars in the data represent the statistical error and the external error bars represent the sum in quadrature of the statistical and systematic errors. The difference between $(4q)$ and twice $(2q)$ is shown in **b**

After the description of the event selection for identified particles at energies up to 189 GeV, the additional criteria for hadron identification are described.

6.1 Event selection at 130 and 136 GeV

After the hadronic preselection described in Sect. 2, events with $\sqrt{s'} > 0.85\sqrt{s}$ were used for further analysis. Data recorded at these two energies were combined and are referred to as the 133 GeV sample. The total of ~ 12 pb^{-1} recorded by DELPHI yields 1387 events while 1406 are expected from simulation.

6.2 Event selection at 161 and 172 GeV

Selected events at 161 GeV were required to have a minimum of 8 and a maximum of 40 charged particles, $\sqrt{s'} > 0.85\sqrt{s}$ and a visible energy of at least 50% of $\sqrt{s}$. A cut was imposed on the polar angle θ of the thrust axis to select events well within the acceptance of the detector. It was found that a selection based on the narrow jet broadening, B_N, is effective in removing the WW events and minimises the bias introduced on the remaining event sample. At threshold about 30 WW events are expected. Selecting events with $B_N \leq 0.12$ reduces this background by 50%.

Using this selection 342 events are expected from simulation, while 357 were selected from the data, with an estimated remaining WW background of 15 events.

At 172 GeV, in addition to the criteria described above, events were required to have at most 38 charged particles and $B_N \leq 0.1$. This leads to 267 selected events, with 264 expected from simulation, out of which 36 are WW background.

6.3 Event selection at 183 and 189 GeV

The event selection for charged identified particles at 189 (183) GeV follows very closely the procedure already described in Sects. 2 and 3. Events with $\sqrt{s'}/\sqrt{s}$ above 0.9 and more than 9(8) charged particles with $p \geq 200$ MeV/c were used. WW background was suppressed by demand-

ing $B_N \leq 0.1(0.08)$. A total of 3617(1122) events were selected with an expected background from WW and Z^0Z^0 of 789 (146) events.

6.4 Selection of charged particles for identification

A further selection was applied to the charged particle sample to obtain *well identifiable* particles. Two different momentum regions were considered, above and below 0.7 GeV/c, which correspond respectively to the separation of samples identified solely by the ionization loss in the Time Projection Chamber (TPC) and by the Čerenkov detectors (RICH) and TPC together. Below 0.7 GeV/c tighter cuts were applied, namely to eliminate secondary protons. There had to be at least 30 wire hits in the TPC associated with the track and the measured track length had be to larger than 100 cm. In addition it was required at least two associated VD layer hits in $r\phi$ and an impact parameter in the $r\phi$ plane of less then 0.1 cm. If there were less than two associated VD layers in z, the corresponding impact parameter had to be less than 1 cm, else less then 0.1 cm. Particles above 0.7 GeV/c were required to have a measured track length bigger than 30 cm and good RICH quality, i.e. presence of primary ionization in the veto regions. Only particles which were well contained in the barrel region of DELPHI ($|\cos(\theta)| \leq 0.7$) were accepted.

6.5 Analysis

For an efficient identification of charged particles over the full momentum region, information from the ionization loss in the TPC ("dE/dx") and information from the DELPHI RICH detectors were combined, using dedicated software packages [26]. One package fine-tunes the Monte Carlo simulation concerning detector related effects (such as slight fluctuations in pressures and refractive indices, background arising from photon feedback, crosstalk between the MWPC readout strips, δ-rays, track ionization photoelectrons, etc.), and another package derives identification likelihoods from the specific energy loss, the number of reconstructed photons and the mean reconstructed Čerenkov angles respectively. The likelihoods are then multiplied and rescaled to one. From these, a set of "tags" which indicate the likelihood for a particular mass hypothesis (π, K, and p) are derived. Throughout this analysis leptons were not separated from pions. Their contribution to the pion sample was subtracted using simulation.

A matrix inversion formalism was used to calculate the true particle rates in the detector from the tagged rates. The 3×3 efficiency matrix is defined by

$$\mathcal{E}_i^j = \frac{\textit{Number of type } i \textit{ hadrons tagged as type } j \textit{ hadrons}}{\textit{Number of type } i \textit{ hadrons}}, \tag{27}$$

where type i, j can be either of π,$K^{\pm}$,p($\overline{\text{p}}$). It establishes the connection between the true particles in the RICH/TPC and the tagged ones:

$$\begin{pmatrix} N_\pi^{meas} \\ N_K^{meas} \\ N_p^{meas} \end{pmatrix} = \mathcal{E} \begin{pmatrix} N_\pi^{true} \\ N_K^{true} \\ N_p^{true} \end{pmatrix} \tag{28}$$

The inverse of the efficiency matrix works on the three sets of tagged particles in two ways. First a particle can have multiple tags, meaning that the information from the tagging is ambiguous. This is not unlikely because in this analysis the low statistics of the data samples force rather loose selection criteria to be applied. Secondly a particle can escape identification. Both effects can be corrected by this method. The average identification efficiency is approximately 85% for pions and 60% for kaons and protons, whereas the purities are approximately 85% and 60% respectively. They show a strong momentum dependence.

K^0 and Λ candidates were reconstructed by their decay in flight into $\pi^+\pi^-$ and pπ^- respectively. Secondary decays candidates, V^0, in the selected sample of hadronic events were found by considering all pairs of oppositely charged particles. The vertex defined by each pair was determined so that the χ^2 of the hypothesis of a common vertex was minimised. The particles were then refitted to the common vertex. The selection criteria were the "standard" ones described in [26]. The average detection efficiency from this procedure is about 36% for the decay $K^0 \rightarrow \pi^+\pi^-$ and about 28% for the decay $\Lambda \rightarrow$ pπ^- in multi-hadronic events. The background under the invariant mass peaks was subtracted separately for each bin of V^0 momentum. The background was estimated from the data by linearly interpolating two sidebands in invariant mass:

- between 0.40 and 0.45 GeV/c^2 and between 0.55 and 0.60 GeV/c^2 for the K^0;
- between 1.08 and 1.10 GeV/c^2 and between 1.14 and 1.18 GeV/c^2 for the Λ.

6.6 Calibration of the efficiency matrix using Z^0 data

The Z^0 data recorded during each year for calibration were used to tune the above described matrix before applying it to high energy data. This is made possible by the fact that studies at the Z^0 pole [34] established that the exclusive particle spectra are reproduced to a very high level of accuracy by the DELPHI-tuned version of the generators. Therefore deviations of the rates of tagged particles between data and simulation in this sample can be interpreted as detector effects. Comparison of the tag rates allows a validation of the efficiency matrix, which would be impossible to measure from the data due to the limited LEP 2 statistics. The matrix is corrected so that it reproduces the simulated rates, assuming that the correction factors are linear in the number of tagged hadrons. The discrepancies were found to be smaller than 4%. This is taken into account when calculating the systematic uncertainties.

As the high energy events are recorded over a long time period, stability of the identification devices becomes a major concern. Variations in the refractive index or

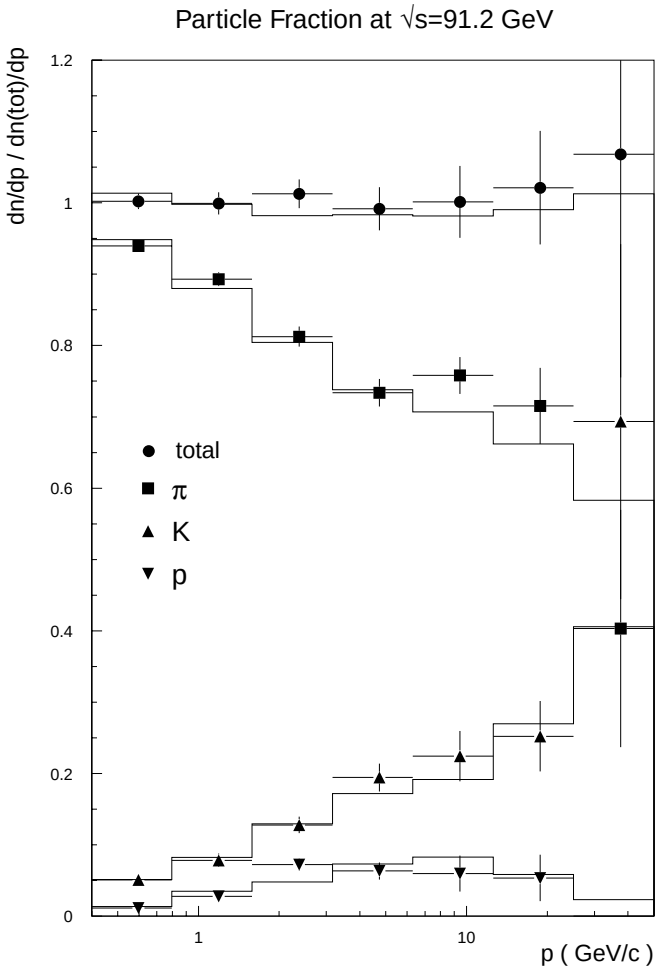

Fig. 8. Fractions of identified particles in radiative Z^0 events from 189 GeV data. The data have been taken under the same conditions as the signal data. Data (points) are in good agreement with the prediction from JETSET (lines) including full detector simulation. The top line and points indicate the sum of the fractions after unfolding. The error bars represent only the statistical error

the drift velocity in the RICH detectors may significantly change the performance of the identification. To estimate the effect of these variations on the measurement, the radiative returns to the Z^0 were used. Such events were selected among the events passing the hadronic preselection, by requiring in addition that they contained at least 8 charged particles, they had $\sqrt{s'} < 130$ GeV, and a total energy transverse to the beam axis of more than 30 GeV. Figure 8 shows the good agreement for differential cross-sections for this event sample which may be taken as an indication of the stability of the detector during the year at the few percent level.

6.7 ξ_p distributions and average multiplicities

After background subtraction, the tagged particle fractions were unfolded using the calibrated matrix. The full covariance matrix was calculated for the tag rates using multinomial statistics. It was then propagated to the true rates of identified particles using the unfolding matrix.

The ξ_p distribution was corrected bin by bin for detector acceptance and selection efficiency, using the full detector simulation. As an example, the corrected ξ_p distributions for charged pions, charged kaons and protons at 189 GeV are shown in Figs. 9,10,11 for $q\bar{q}$, $(4q)$ and $(2q)$ events respectively. In the figures the predictions from the DELPHI simulation as well as a fit to expression (3), if the fit converged, are also shown. Figure 12 shows the same distributions for K^0 and Λ in $q\bar{q}$ events at 183 and 189 GeV. Within the statistics of the data samples analysed, the shapes of the ξ_p distributions are reasonably well described by the generators, with the exception of the K^0 for which the agreement is poorer.

The multiplicity of the identified final states per hadronic event was obtained by integration of the corresponding ξ_p distributions. The results are shown in Table 2. The numbers given for charged identified hadrons include decay products from particles with a lifetime $\tau < 10^{-9}$ s. These numbers are compared with the predictions from PYTHIA 5.7, HERWIG 5.8 and ARIADNE 4.8.

The following sources of systematic uncertainties are taken into account.

1. Uncertainties due to particle identification.
   They are mainly due to the uncertainties in the modelling of the detector response. In addition for the charged particles there are time dependent effects such as variations of the drift velocity in the RICH detectors.
   The unfolding matrix was adjusted using the Z^0-calibration data recorded in the beginning of data taking in 1996, 1997 and 1998, as well as from the peak period in 1995. This is described in Sect. 6.6. For 1997 and 1998 data also radiative return Z^0-events were used. These are better suited as they were recorded under the same conditions as the signal events.
   Spectra were obtained using the original and the adjusted matrices. The difference between the results obtained was taken as the corresponding systematic uncertainty.
   The relative size of this uncertainty, averaged over the centre-of-mass energies is 0.006, 0.076 and 0.136 for charged pions, kaons and protons respectively.
   A relative systematic uncertainty of 3% was estimated for K^0 [35] and 5% for Λ [36].
2. Size of the subtracted WW background (where applicable).
   Variation of the selection criteria results in a 10% uncertainty on the fraction of the W contamination in the $q\bar{q}$ sample. This corresponds to a 5% uncertainty in the W cross-section and the size of the W background has been varied accordingly. The maximal variation observed in the distributions has been taken as the corresponding systematic uncertainty. The relative size of this uncertainty, averaged over the centre-of-mass energies is 0.003, 0.010 and 0.003 for charged pions, kaons and protons respectively, and is 0.014 (0.028, negligi-

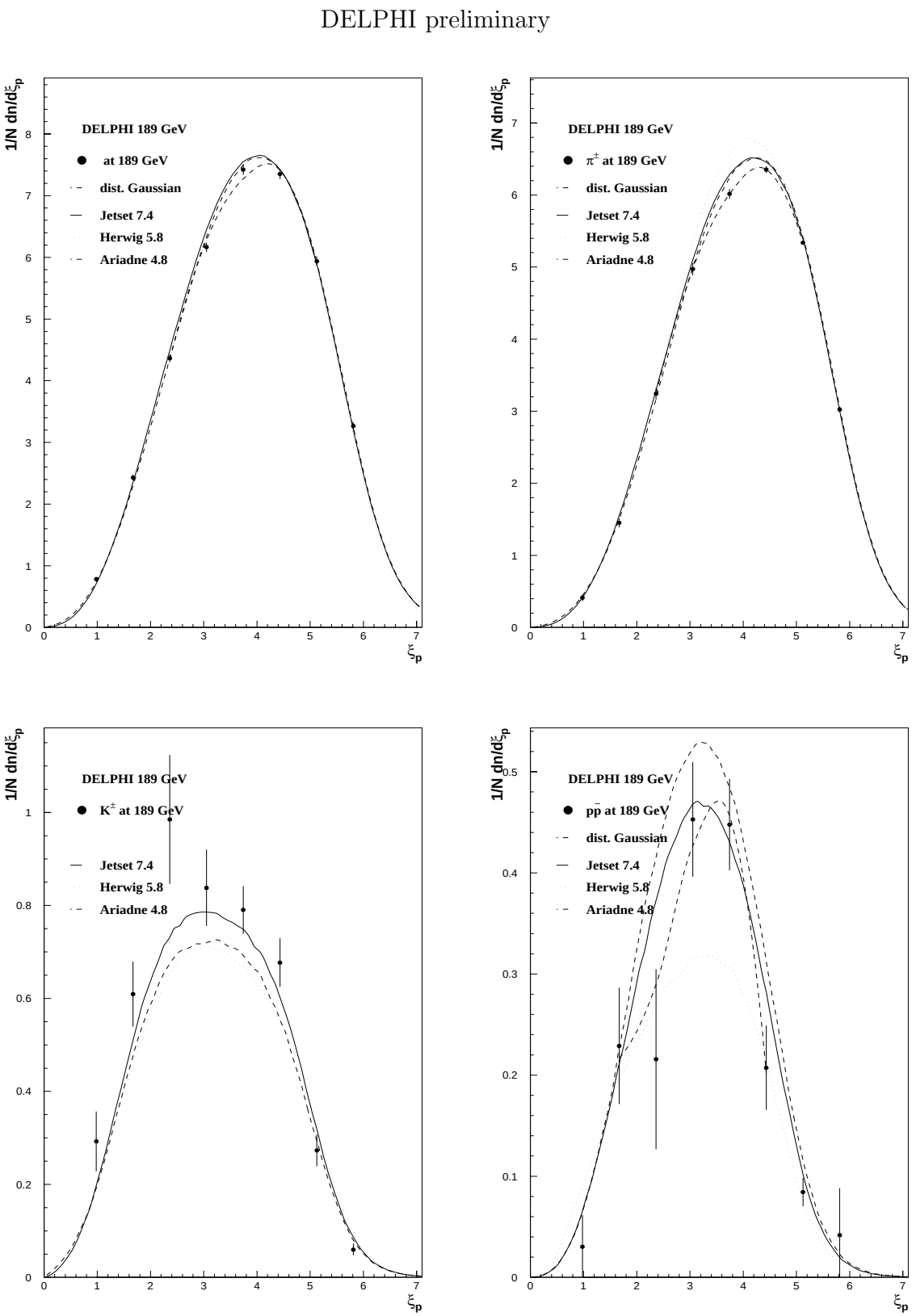

Fig. 9. ξ_p distributions (efficiency corrected and background subtracted) for charged particles, pions, kaons and protons in $q\bar{q}$ events at 189 GeV. Data (points) are compared to the prediction from JETSET (solid line). Only the statistical uncertainties are shown. The dashed dotted line shows a fit to (3)

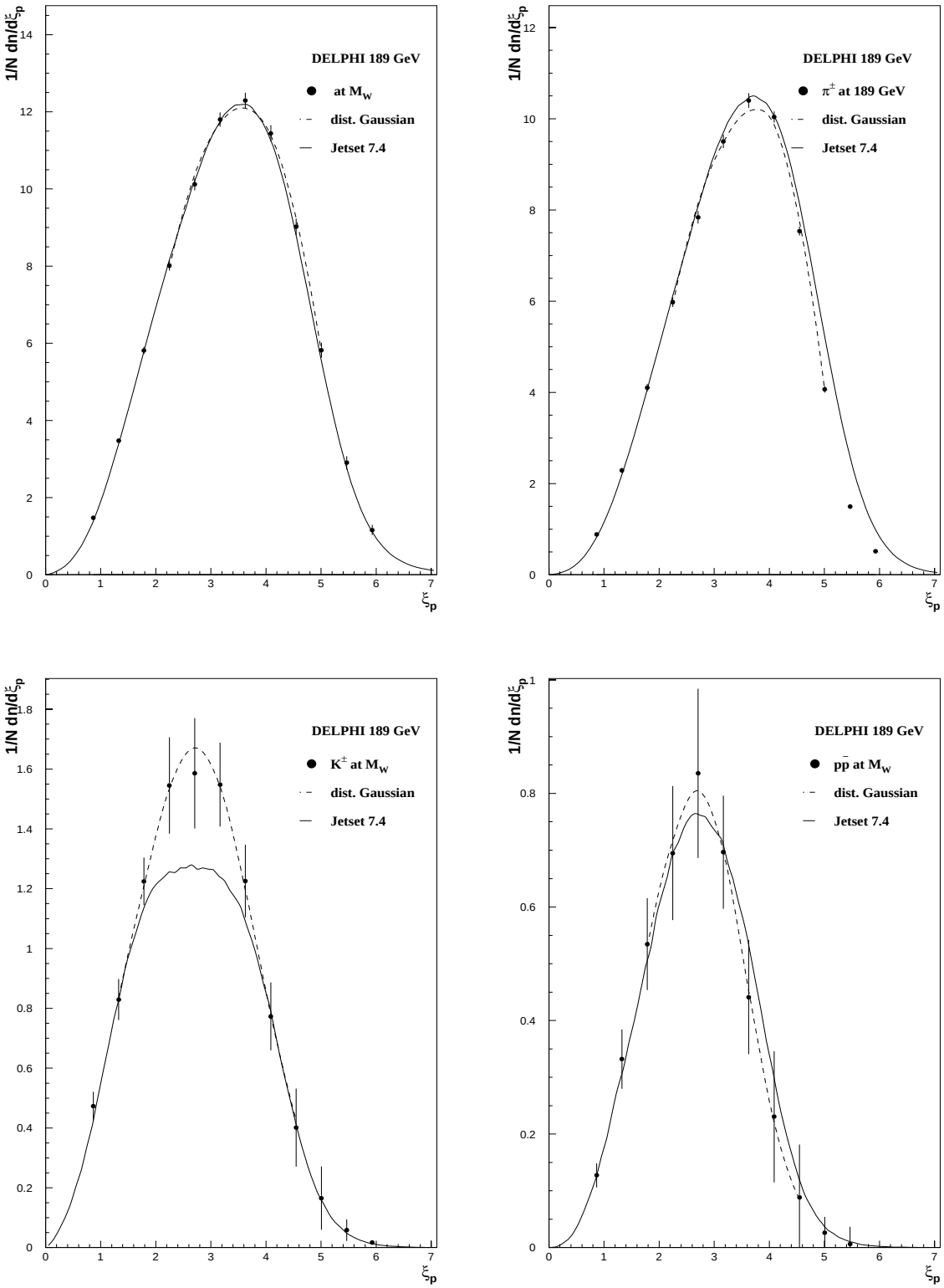

Fig. 10. ξ_p distributions (efficiency corrected and background subtracted) for charged particles, pions, kaons and protons in fully hadronic WW events at 189 GeV. Data (points) which have been boosted back to the W rest-frame, compared to the prediction from JETSET (solid line). Only the statistical uncertainties are shown. The dashed dotted line shows a fit to (3)

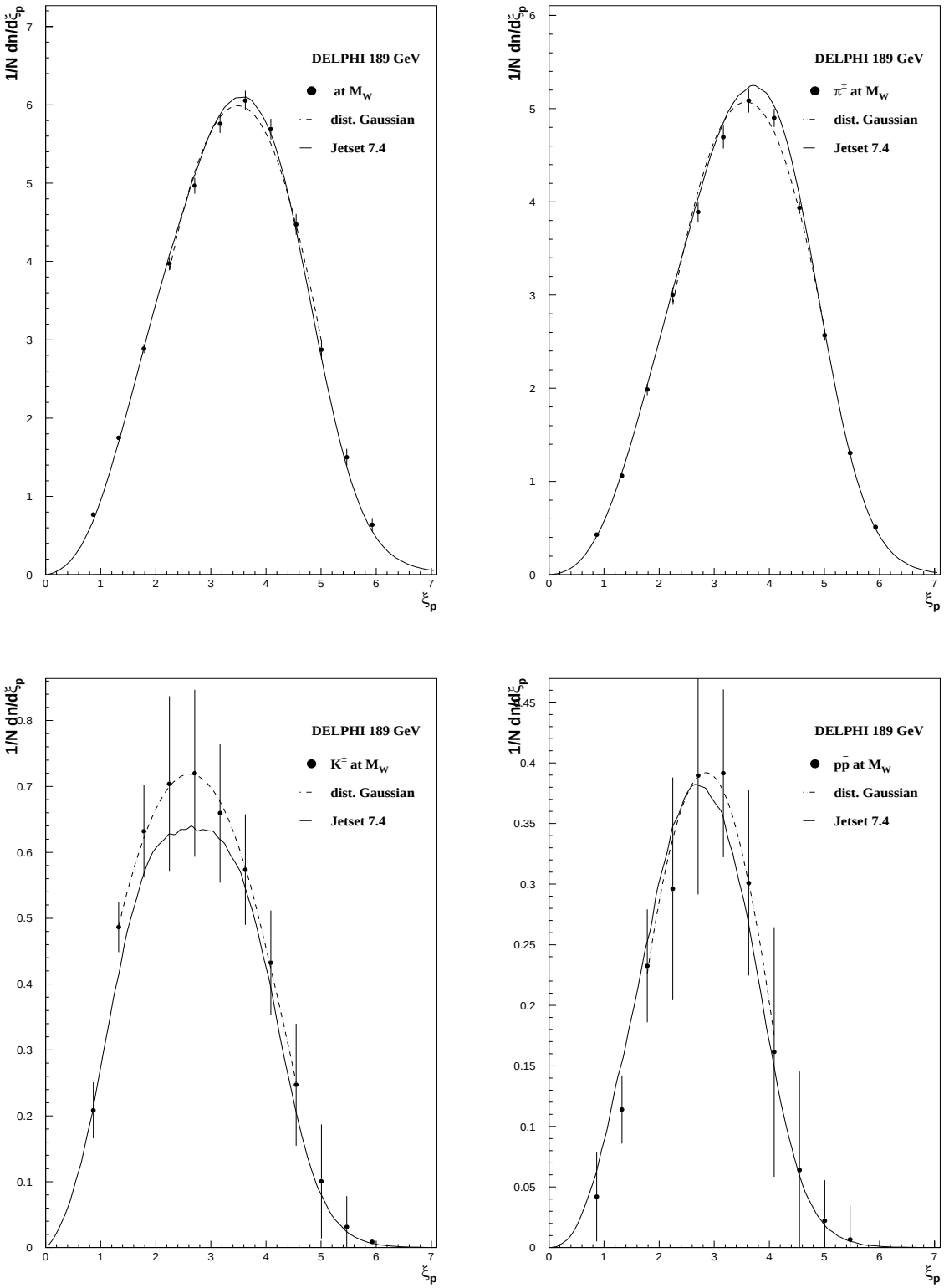

Fig. 11. ξ_p distributions (efficiency corrected and background subtracted) for charged particles, pions, kaons and protons in semileptonic WW events at 189 GeV. Data (points) which have been boosted back to the W rest-frame, compared to the prediction from JETSET (solid line). Only the statistical uncertainties are shown. The dashed dotted line shows a fit to (3)

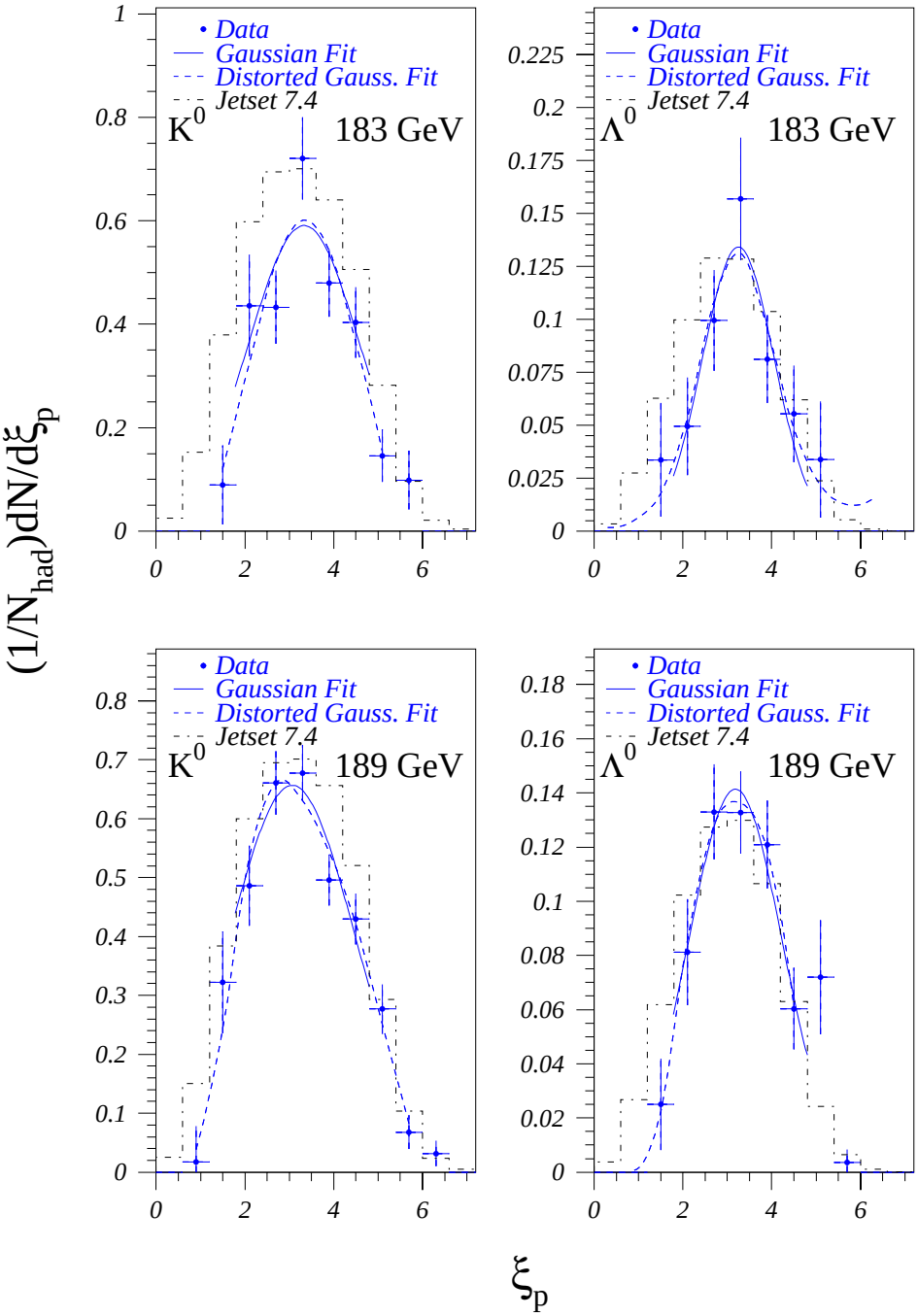

Fig. 12. ξ_p distributions (efficiency corrected and background subtracted) for neutral Kaons and neutral Lambdas in $e^+e^- \to q\bar{q}$ at 183 GeV and 189 GeV respectively, for data (points), and simulation using JETSET (dashed-dotted histogram). The full curves show the fit of the data to a Gaussian and the dashed ones to a distorted Gaussian. The error bars represent only the statistical error

ble) and 0.032 (0.057) for K^0 and Λ, respectively, at centre of mass energies of 189 (183, 161) GeV.

3. Particles with momenta below 0.2 GeV/c or above 50 GeV/c were not identified. Their contribution was extrapolated from the simulation. Half of the extrapolated multiplicity was added in quadrature to the systematic uncertainty. The relative size of this uncertainty, averaged over the centre-of-mass energies is 0.021, 0.003 and 0.001 for charged pions, kaons and protons respectively, while for K^0 and Λ at 133 GeV, 183 GeV and 189 GeV, is 0.034, and for K^0 at 161 GeV is 0.042.
4. For the pions this analysis relies on a subtraction of the lepton contamination using simulation.
   An extra uncertainty of 10% of the simulation prediction for the total number of leptons is added. The relative size of this uncertainty, averaged over the centre-of-mass energies is 0.003.

In Fig. 13 the results are compared to the predictions from PYTHIA 5.7 and HERWIG 5.8. The results shown for energies below 133 GeV (open squares) were extracted from reference [29]. The models account for the measurements, with the exception of the HERWIG predictions for

Table 2. Average multiplicities of particles π^+, K^+, K^0, p and Λ at 133, 161, 172, 183 and 189 GeV. The first uncertainty is statistical and the second is systematic

$\sqrt{s}$ [GeV]	Particle	$\langle n \rangle$			
		PYTHIA 5.7	HERWIG 5.8	ARIADNE 4.8	Data
133	$\pi^\pm$	19.90	19.97	19.64	$19.84 \pm 0.29 \pm 0.44$
	$K^\pm$	2.37	2.32	2.30	$2.60 \pm 0.26 \pm 0.13$
	K^0	2.40	2.64		$2.51 \pm 0.21 \pm 0.11$
	$p\bar{p}$	1.11	0.89	1.29	$1.56 \pm 0.25 \pm 0.09$
	Λ	0.34	0.49		$0.50 \pm 0.07 \pm 0.03$
161	$\pi^\pm$	21.24	21.76	21.12	$20.75 \pm 0.58 \pm 0.50$
	$K^\pm$	2.63	2.44	2.44	$2.87 \pm 0.55 \pm 0.25$
	K^0	2.56	2.78		$2.65 \pm 0.34 \pm 0.14$
	$p\bar{p}$	1.26	0.96	1.40	$1.21 \pm 0.48 \pm 0.02$
	Λ				
172	$\pi^\pm$	21.77	22.31	21.68	$21.79 \pm 0.68 \pm 0.47$
	$K^\pm$	2.68	2.48	2.50	$2.09 \pm 0.74 \pm 0.29$
	K^0				
	$p\bar{p}$	1.30	0.99	1.45	$1.78 \pm 0.73 \pm 0.25$
	Λ				
183	$\pi^\pm$	22.28	22.82	21.18	$21.79 \pm 0.36 \pm 0.46$
	$K^\pm$	2.74	2.53	2.55	$2.83 \pm 0.37 \pm 0.13$
	K^0	2.66	2.91		$1.81 \pm 0.14 \pm 0.10$
	$p\bar{p}$	1.33	1.00	1.48	$1.32 \pm 0.34 \pm 0.17$
	Λ	0.39	0.55		$0.33 \pm 0.04 \pm 0.03$
189	$\pi^\pm$	22.56	23.10	22.47	$22.19 \pm 0.24 \pm 0.46$
	$K^\pm$	2.77	2.55	2.57	$3.15 \pm 0.21 \pm 0.24$
	K^0	2.67	2.93		$2.10 \pm 0.12 \pm 0.10$
	$p\bar{p}$	1.35	1.02	1.50	$1.19 \pm 0.17 \pm 0.41$
	Λ	0.39	0.56		$0.40 \pm 0.03 \pm 0.03$

K^0 and Λ and of the PYTHIA predictions for K^0 at high energy which are above the measured values.

6.8 ξ^* and its evolution

An interesting aspect of the ξ_p-distribution is the evolution of its peak position ξ^* with increasing centre-of-mass energy. It is determined by fitting a parametrisation of the distribution to the peak region.

One such parametrisation is the distorted Gaussian in (3). Another parametrisation is a standard Gaussian distribution. While being a more crude approximation, it facilitates the analysis in the case of limited statistics.

Since (3) is expected to describe well only the peak region, the fit range has to be carefully chosen around the peak. Table 3 shows the results and the fit range, with the χ^2 per degree of freedom for the gaussian fit, except for the K^0 and Λ at 133 GeV where only the distorted gaussian fit was performed. The errors in the data are the sum in quadrature of the statistical and systematic uncertainties (generator values were extracted from samples of one million events generated with the DELPHI tuned versions of the programs).

The systematic uncertainty has the following contributions which were added in quadrature to the statistical uncertainty of the fit.

1. Uncertainty of the background evaluation (above the W threshold).
   This source was evaluated as the maximal difference obtained by a variation of the WW background cross-section.
   The relative size of this uncertainty, averaged over the centre-of-mass energies is 0.005, 0.010, 0.002, 0.024 and 0.023 for charged pions, kaons, protons, K^0 and Λ respectively.
2. Uncertainty due to the particle identification.
   The analysis was repeated using the calibrated matrices or changes by 3% (K^0) or 5% (Λ) in the bin contents of the ξ_p distribution, and the fit redone. The maximal differences in the position of the peak thus obtained were added in quadrature.
   The relative size of this uncertainty, averaged over the centre-of-mass energies is 0.011, 0.017, 0.002, 0.019 and

Table 3. Values of ξ^* for π^+, K^+, K^0, p and Λ in $e^+e^- \to q\bar{q}$ at 133, 161, 172, 183 and 189 GeV. The errors are the sum in quadrature of the statistical and the total systematic uncertainties, and the χ^2/ndf corresponds to the Gaussian fit, except for K^0 and Λ at 133 GeV

$\sqrt{s}$		fit range		PYTHIA		HERWIG		ARIADNE		Data		
		Gauss.	dist. G.	Gauss.	dist. G.	Gauss.	dist. G.	Gauss.	dist. G.	Gauss.	χ^2/ndf	dist. G.
133	$\pi^\pm$	[3.3 : 4.9]	[2.5 : 5.5]	3.90	4.11	3.90	4.12	4.00	4.15	4.04 ± 0.13	0.017	4.32 ± 0.37
	$K^\pm$	[2.1 : 3.3]		2.85	2.99	2.86	2.99	2.85	2.99	2.90 ± 0.30	1.39	
	K^0		[0.6 : 5.4]		2.87		3.15				1.63	2.86 ± 0.43
	$p\bar{p}$	[2.1 : 3.3]		3.04	3.09	3.04	3.10	3.04	3.04	2.74 ± 0.33	1.86	
	Λ		[0.6 : 4.8]		2.79		2.99				3.22	2.81 ± 0.66
161	$\pi^\pm$	[3.5 : 5.1]	[2.6 : 4.5]	4.09	4.17	4.03	4.08	4.12	4.18	4.11 ± 0.15	1.10	4.14 ± 0.48
	$K^\pm$	[2.1 : 3.7]		2.99	2.98	3.00	3.00	3.01	2.98	3.16 ± 0.50	0.57	
	K^0											
	$p\bar{p}$	[2.1 : 3.7]		3.01	3.14	3.20		3.14	3.06	3.08 ± 0.84	1.1	
	Λ											
172	$\pi^\pm$	[3.5 : 5.1]	[2.6 : 5.5]	4.13	4.20	4.06	4.12	4.16	4.21	4.11 ± 0.14	1.07	4.45 ± 0.40
	$K^\pm$	[2.1 : 3.7]		3.04	3.02	3.03	3.01	3.05	3.01	2.98 ± 0.84	1.76	
	K^0											
	$p\bar{p}$	[2.1 : 3.7]		3.16	3.14	3.23	3.41	3.18	3.12	3.55 ± 1.10	0.98	
	Λ											
183	$\pi^\pm$	[2.6 : 4.5]	[3.5 : 5.1]	4.16	4.43	4.10	4.30	4.19	4.44	4.23 ± 0.13	2.8	4.63 ± 0.20
	$K^\pm$	[2.1 : 3.7]		3.08	3.18	3.06	3.15	3.10	3.23	3.08 ± 0.29	1.19	
	K^0	[1.8 : 4.8]	[1.2 : 5.4]	3.09	3.19					3.33 ± 0.63	2.75	3.35 ± 0.63
	$p\bar{p}$	[2.3 : 3.7]	[2.1 : 3.7]	3.21	3.32	3.31		3.21	3.39	3.29 ± 0.18	0.98	3.29 ± 0.52
	Λ	[1.8 : 4.8]	[0.6 : 6.6]	3.02	3.01					3.25 ± 0.51	0.87	3.22 ± 0.51
189	$\pi^\pm$	[2.6 : 4.5]		4.22		4.08				4.18 ± 0.10	2.32	
	$K^\pm$	[2.1 : 4.7]		3.17		3.08				3.10 ± 0.25	0.26	
	K^0	[1.8 : 4.8]	[0.6 : 6.0]	3.13	3.02					3.06 ± 0.48	1.66	2.81 ± 0.43
	$p\bar{p}$	[2.1 : 4.7]		3.11		3.20				3.18 ± 0.12	0.01	
	Λ	[1.8 : 4.8]	[0.6 : 4.8]	3.02	2.98					3.18 ± 0.48	0.38	3.21 ± 0.49

0.017 for charged pions, kaons, protons, K^0 and Λ respectively.

3. Stability of the fit and dependence on the fit range.
   To estimate this effect, which arises from the combination of the limited statistics, the resulting need to choose a coarse binning, and the choice of the fit range, systematic shifts have been imposed on the data by variation within the statistical uncertainty. One standard deviation has been added to the values left of the peak and one standard deviation has been subtracted from the values to its right and vice versa. The maximum variation is taken as the contribution to the systematic uncertainty.
   The relative size of this uncertainty, averaged over the centre-of-mass energies is 0.026, 0.112, 0.161, 0.163 and 0.147 for charged pions, kaons, protons, K^0 and Λ respectively.

Figure 14 shows the ξ^* values from the Gaussian fits as a function of the centre-of-mass energy. The data up to centre-of-mass energies of 91 GeV were taken from previous measurements [37]. The fits to expression (4), with Y and $C = 0.351$ defined as in (5) and F_h and Λ_{eff} taken as free parameters, were done separately for each particle type and are superimposed on the data points (lines). Figure 14 shows that (within the statistics of the data samples analysed) the fitted functions follow well the data points. This suggests that MLLA+LPHD gives a good description of the observed particle spectra. From Table 3 it is shown that there is fair agreement between the data and the predictions from the generators (PYTHIA 5.7, HERWIG 5.8, and ARIADNE 4.8).

7 Identified hadrons in WW events

The selections of $(4q)$ and $(2q)$ WW events in the analysis of identified hadrons in WW events at 189 GeV are similar to the procedures described in [38]. A feed forward neural network, trained with back-propagation on PYTHIA simulated events, was used to improve the separation of $(4q)$ WW events from 2-fermion (mainly $Z^0/\gamma \to q\bar{q}(\gamma)$) and 4-fermion background (mainly Z^0Z^0 events). The network input variables, the training procedure and its per-

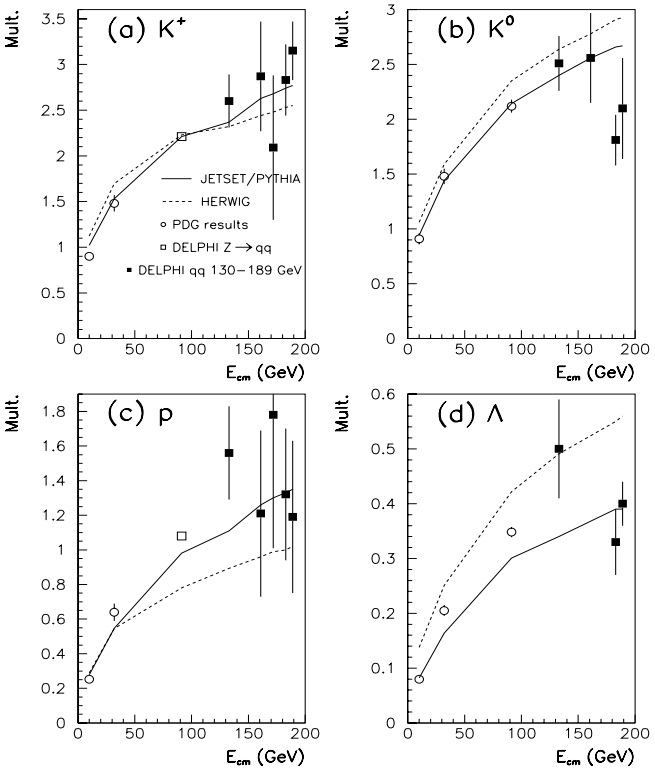

Fig. 13a–d. Average multiplicity of K^+ **a**, K^0 **b**, p **c** and Λ **d** as function of the centre-of-mass energy. Black squares are DELPHI high energy data, open squares are measurements from a previous DELPHI publication [34], and open bullets are values taken from the PDG [29]. Simulations using PYTHIA tuned to DELPHI data (solid line) and HERWIG 5.8 (dashed line) are superimposed. The error bars represent the sum in quadrature of the statistical and the systematic uncertainties

formance are described in detail in [38]. The purities and the selection efficiencies were determined from the simulation to be respectively 73% and 83% in the $(4q)$ sample and 89% and 75% in the $(2q)$ sample.

7.1 ξ_p distributions for identified particles at M_W

The mass of the W boson is the relevant energy scale which enters in the ξ_p variable; it is thus appropriate to compute the ξ_p distributions and their peak positions from W decays after a boost to the rest frame of the W. The boosting procedure relies on the simulation for the part of the spectrum which was not accessible before the boosting, and thus introduces a certain model dependence. This does not affect significantly the peak region, which is used to extract ξ^*. Figure 11 shows the ξ_p distributions obtained from semi-leptonic W events.

Table 4 shows the values of ξ^* for the semi-leptonic W data at 189 GeV and for the WW simulation. The ξ^* values were obtained by a Gaussian fit in the indicated region. The systematic uncertainties were estimated in the same way as described in the previous section. The relative uncertainty due to particle identification is 0.03, 0.05 and 0.05 for charged pions, kaons and protons respectively. The relative uncertainty due to stability evaluation of the fit is 0.06, 0.12 and 0.15 for charged pions, kaons and protons.

Table 4. Values for ξ^* for $\pi^\pm$, $K^\pm$ and protons from a Gaussian fit to the semi-leptonic W data at 189 GeV. The fit was made to the spectra in the W rest frame. The first error is statistical and the second reflects the total systematic uncertainties. Also indicated is the $\chi^2/n.d.f$

	fit range	WW simulation	data	$\chi^2/n.d.f.$
$\pi^\pm$	[2.7 : 4.5]	3.66	$3.65 \pm 0.02 \pm 0.24$	1.20/2
$K^\pm$	[1.10 : 3.86]	2.70	$2.61 \pm 0.09 \pm 0.33$	0.02
$p\bar{p}$	[1.10 : 3.86]	2.73	$2.86 \pm 0.11 \pm 0.44$	0.08

Within the limited statistics of this sample the data are in good agreement with the generator prediction as well as with the prediction from MLLA (4).

7.2 Average multiplicity

After the event selection the analysis proceeds along the same lines as described for the $q\bar{q}$ analysis. Fully corrected ξ_p-distributions are obtained and afterwards integrated to obtain the multiplicity. The results for the average multiplicity are shown in Table 5 and compared to the predictions from PYTHIA 5.7 and HERWIG 5.8, with the systematic errors estimated as in Sect. 6.7. The relative size of the systematic uncertainty due to extrapolation into the unseen region is 0.023 (0.024), 0.0023 (0.0022) and 0.0011 (0.0011) for charged pions, kaons and protons from fully hadronic (semi-leptonic) W decays. The relative size of the systematic uncertainty due to particle identification is 0.0052 (0.0093), 0.026 (0.076) and 0.088 (0.59) for charged pions, kaons and protons from fully hadronic (semi-leptonic) W decays. Finally, the relative size of the systematic uncertainty due to uncertainty in the estimate of the subtracted background is 0.0013 (0.0003), 0.0027 (0.0004) and 0.0022 (0.0011) for charged pions, kaons and protons from fully hadronic (semi-leptonic) W decays.

The ratios of the average multiplicities in (4q) events to twice the multiplicities in (2q) events for different hadron species, conservatively assuming uncorrelated errors, for the full momentum range and for momentum between 0.2 and 1.25 GeV/c are shown in Table 6, and are compatible with unity. The systematic errors for the restricted momentum range were assumed to be proportional to the sum in quadrature of the systematic errors in the full momentum range, excluding the contributions from the extrapolation.

8 Summary and discussion

The mean charged particle multiplicities $\langle n \rangle$ and dispersions D in $q\bar{q}$ events at the different centre-of-mass energies were measured to be:

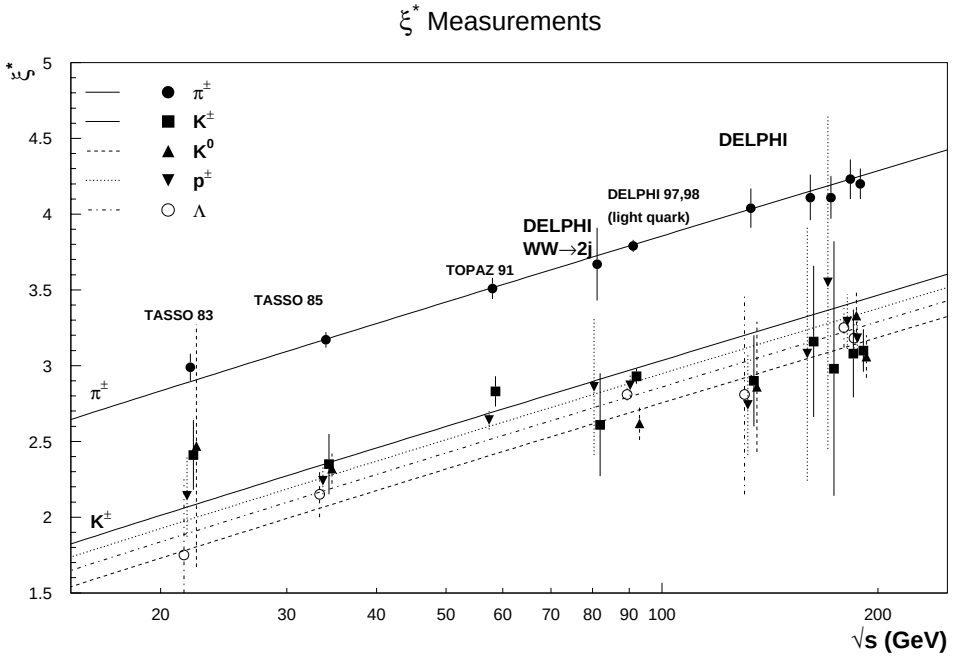

Fig. 14. Evolution of ξ^* in $e^+e^- \to q\bar{q}$ with increasing centre-of-mass energy. This measurement is compared with previous measurements from DELPHI from [34] and lower energy experiments [37]. The lines are fits to (4) for the hadrons listed in the figure. The error bars represent the sum in quadrature of the statistical and the systematic uncertainties. For better legibility the data points have been shifted from the nominal energy

Table 5. Average multiplicity for $\pi^{\pm}$, $K^{\pm}$ and protons for WW events at 189 GeV. In the data the first uncertainty is statistical and the second is systematic

event type	Particle	$\langle n \rangle$ (Data)	$\langle n \rangle$ PYTHIA 5.7	$\langle n \rangle$ HERWIG 5.8
WW $\to q\bar{q}q\bar{q}$	$\pi^{\pm}$	$31.65 \pm 0.48 \pm 0.76$	31.74	31.55
	$K^{\pm}$	$4.38 \pm 0.42 \pm 0.12$	4.05	3.63
	$p\bar{p}$	$1.82 \pm 0.29 \pm 0.16$	1.89	1.66
WW $\to q\bar{q}l\nu$	$\pi^{\pm}$	$15.51 \pm 0.38 \pm 0.40$	15.90	16.08
	$K^{\pm}$	$2.23 \pm 0.32 \pm 0.17$	2.02	1.82
	$p\bar{p}$	$0.94 \pm 0.23 \pm 0.06$	0.95	0.83

Table 6. Ratio of average multiplicities in (4q) events to twice the values in (2q) events for $\pi^{\pm}$, $K^{\pm}$ and protons from WW events at 189 GeV, for different momentum ranges. The first uncertainty is statistical and the second is systematic

Particle	$\langle n \rangle(4q)/(2 \cdot \langle n \rangle(2q))$	
	All p	0.2 GeV/c $< p <$ 1.25 GeV/c
$\pi^{\pm}$	$1.02 \pm 0.03 \pm 0.04$	$1.03 \pm 0.03 \pm 0.01$
$K^{\pm}$	$0.98 \pm 0.17 \pm 0.08$	$0.96 \pm 0.38 \pm 0.08$
$p\bar{p}$	$0.97 \pm 0.28 \pm 0.11$	$0.72 \pm 0.57 \pm 0.08$

$$\langle n \rangle_{183\,\mathrm{GeV}} = 27.05 \pm 0.27(stat) \pm 0.32(syst) \quad (29)$$
$$D_{183\,\mathrm{GeV}} = 8.08 \pm 0.19(stat) \pm 0.14(syst) \quad (30)$$
$$\langle n \rangle_{189\,\mathrm{GeV}} = 27.47 \pm 0.18(stat) \pm 0.30(syst) \quad (31)$$
$$D_{189\,\mathrm{GeV}} = 8.77 \pm 0.13(stat) \pm 0.11(syst) \quad (32)$$
$$\langle n \rangle_{200\,\mathrm{GeV}} = 27.58 \pm 0.19(stat) \pm 0.45(syst) \quad (33)$$
$$D_{200\,\mathrm{GeV}} = 8.64 \pm 0.13(stat) \pm 0.20(syst)\,. \quad (34)$$

Figure 15 shows the value of the average charged particle multiplicity in $e^+e^- \to q\bar{q}$ events at 183, 189 and 200 GeV compared with lower energy points from JADE [39], PLUTO [40], MARK II [41], TASSO [42], HRS [43], and AMY [44], with DELPHI results in $q\bar{q}\gamma$ events at the Z^0 [45], with the world average at the Z^0 [29], and with LEP results at high energy [46–54]. The points from JADE, PLUTO and MARK II do not include the decay products of short lived K^0 and Λ. The value at M_{Z^0} has been lowered by 0.20 to account for the different proportion of $b\bar{b}$ and $c\bar{c}$ events at the Z^0 with respect to the $e^+e^- \to \gamma^* \to q\bar{q}$ [55]. Similarly, the values at 133, 161, 172, 183 and 189 GeV were lowered by 0.15, 0.12, 0.11, 0.08, 0.05 and 0.07 respectively. The QCD prediction for the charged particle multiplicity has been computed as a function of α_s including the resummation of leading (LLA) and next-to-leading (NLLA) corrections [56]:

$$\langle n \rangle(\sqrt{s}) = a[\alpha_s(\sqrt{s})]^b e^{c/\sqrt{\alpha_s(\sqrt{s})}} \left[1 + O(\sqrt{\alpha_s(\sqrt{s})})\right] , \quad (35)$$

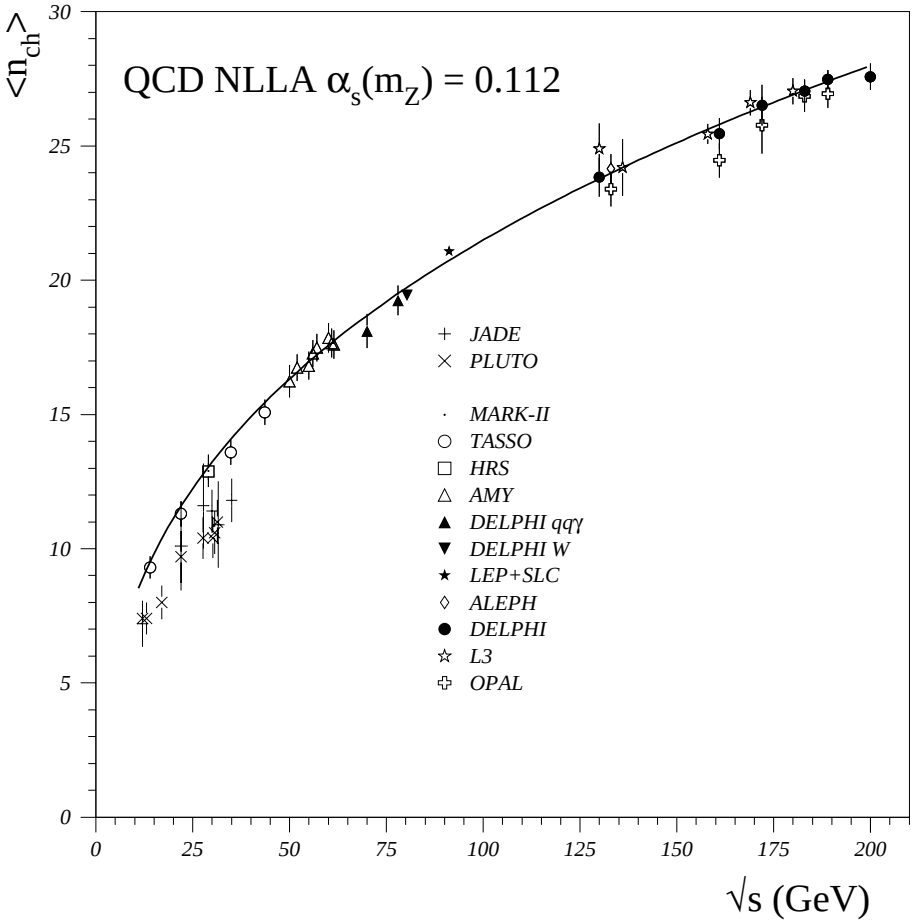

Fig. 15. Measured average charged particle multiplicity in $e^+e^- \to q\bar{q}$ events as a function of centre-of-mass energy $\sqrt{s}$. DELPHI high energy results are compared with other experimental results and with a fit to a prediction from QCD in Next to Leading Order. The error bars represent the sum in quadrature of the statistical and the systematic uncertainties. Some points are slightly shifted on the abscissa for clarity. The average charged multiplicity in W decays is also shown at an energy corresponding to the W mass. The measurements have been corrected for the different proportions of $b\bar{b}$ and $c\bar{c}$ events at the various energies

where s is the squared centre-of-mass energy and a is a parameter (not calculable from perturbation theory) whose value has been fitted from the data. The constants $b = 0.49$ and $c = 2.27$ are predicted by theory [56] and $\alpha_s(\sqrt{s})$ is the strong coupling constant. The fitted curve to the data between 14 GeV and 200 GeV, excluding the results from JADE, PLUTO and MARK II, is plotted in Fig. 15, corresponding to $a = 0.045$ and $\alpha_s(m_Z) = 0.112$. The multiplicity values are consistent with the QCD prediction on the multiplicity evolution with centre-of-mass energy.

The ratios of the average multiplicity to the dispersion measured at 183 GeV, 189 GeV and 200 GeV, $\langle n \rangle / D = 3.35 \pm 0.11$, $\langle n \rangle / D = 3.14 \pm 0.07$ and $\langle n \rangle / D = 3.19 \pm 0.10$ (where the errors are the sum in quadrature of the statistical and of the systematic) respectively, are consistent with the weighted average from the measurements at lower centre-of-mass energies (3.13 ± 0.04), as can be seen in Fig. 16. From Koba-Nielsen-Olesen scaling [57] this ratio is predicted to be energy-independent. The ratio measured is also consistent with the predictions of QCD including 1-loop Higher Order terms (H.O.) [58].

For WW events the measured multiplicities in the fully hadronic channel are:

$$\langle n^{(4q)} \rangle_{189\,\mathrm{GeV}} = 39.12 \pm 0.33(stat) \pm 0.36(syst) \quad (36)$$

$$\langle n^{(4q)} \rangle_{183\,\mathrm{GeV}} = 38.11 \pm 0.57(stat) \pm 0.44(syst)\,, \quad (37)$$

while for the semileptonic channel they are:

$$\langle n^{(2q)} \rangle_{189\,\mathrm{GeV}} = 19.49 \pm 0.31(stat) \pm 0.27(syst) \quad (38)$$

$$\langle n^{(2q)} \rangle_{183\,\mathrm{GeV}} = 19.78 \pm 0.49(stat) \pm 0.43(syst)\,. \quad (39)$$

The PYTHIA Monte Carlo program with parameters tuned to the DELPHI data at LEP 1, predicts multiplicities of 38.2 and 19.1 for the fully hadronic and semileptonic events respectively.

A possible depletion of the multiplicity in fully hadronic WW events with respect to twice the semileptonic events, as predicted by most colour reconnection models, is not observed in the full momentum range, in agreement with the results from other LEP collaborations [59]:

$$\left(\frac{\langle n^{(4q)} \rangle}{2\langle n^{(2q)} \rangle} \right) = 0.990 \pm 0.015(stat) \pm 0.011(syst)\,, \quad (40)$$

nor in the momentum range $0.1 < p < 1.0$ GeV/c:

$$\left. \frac{\langle n^{(4q)} \rangle}{2\langle n^{(2q)} \rangle} \right|^{0.1<p<1\,GeV/c} = 0.981 \pm 0.024(stat) \pm 0.013(syst). \quad (41)$$

No significant difference is observed between the dispersion in fully hadronic events and $\sqrt{2}$ times the dispersion in semileptonic events:

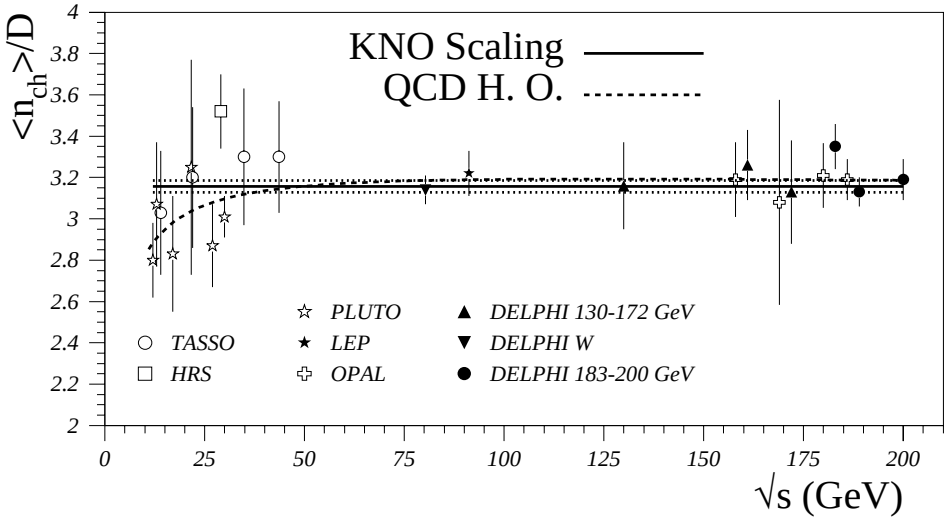

Fig. 16. Ratio of the average charged particle multiplicity to the dispersion in $e^+e^- \to q\bar{q}$ events at 183, 189 and 200 GeV, compared with lower energy measurements. The error bars represent the sum in quadrature of the statistical and the systematic uncertainties. Some points are slightly shifted on the abscissa for clarity. The ratio in W decays is also shown at an energy corresponding to the W mass. The straight solid and dotted lines represent the weighted average of the data points and its error. The dashed line represents the prediction from QCD (see text)

$$\frac{D^{(4q)}}{\sqrt{2}D^{(2q)}} = 0.94 \pm 0.03(\text{stat}) \pm 0.03(\text{syst})\,.$$

Assuming uncorrelated systematic errors for the two centre-of-mass energies, 183 and 189 GeV, the inverse of the sums in quadrature of the statistical and the systematic errors were used as weights to give the averages:

$$\langle n^{(W)} \rangle = 19.44 \pm 0.13(stat) \pm 0.12(syst) \qquad (42)$$

$$D^{(W)} = 6.20 \pm 0.11(stat) \pm 0.06(syst)\,, \qquad (43)$$

where the multiplicities and their errors in (4q) were divided by 2 and the dispersions and their errors in (4q) were divided by $\sqrt{2}$.

The value of $\langle n^{(W)} \rangle$ is plotted in Fig. 15 at an energy value corresponding to the W mass, with an increase of 0.35 applied to account for the different proportion of events with a b or a c quark. The measurement lies on the same curve as the neutral current data. The value of $\langle n^{(W)} \rangle / D^{(W)} = 3.14 \pm 0.07(stat+syst)$, plotted in Fig. 16, is also consistent with the $e^+e^- \to \gamma^* \to q\bar{q}$ average.

The production of π^+, K^+, K^0, p and Λ from $q\bar{q}$ and WW events at 189 GeV was also studied. The results on the average multiplicity of identified particles and on the position ξ^* of the maximum of the $\xi_p = -\log(\frac{2p}{\sqrt{s}})$ distribution were compared with predictions of PYTHIA and with calculations based on MLLA+LPHD approximations. Within their uncertainties the data are in good agreement with the prediction from the generator as well as with the predictions based on the analytical calculations in the MLLA framework.

The ratio of the multiplicities of identified heavy hadrons in (4q) events to twice those in (2q) events is compatible with unity, both for the full momentum range and momenta between 0.2 and 1.25 GeV/c:

Particle	All p	0.2 GeV/c $< p <$ 1.25 GeV/c
$K^\pm$	$0.98 \pm 0.17 \pm 0.08$	$0.96 \pm 0.38 \pm 0.08$
$p\bar{p}$	$0.97 \pm 0.28 \pm 0.11$	$0.72 \pm 0.57 \pm 0.08$.

The evolution for the ξ^* for identified hadrons is in good agreement with the prediction from perturbative QCD (4). This underlines the applicability of MLLA/LPHD for the description of hadron production in e^+e^- annihilation over the full LEP energy range.

Acknowledgements. We are greatly indebted to our technical collaborators, to the members of the CERN-SL Division for the excellent performance of the LEP collider, and to the funding agencies for their support in building and operating the DELPHI detector. We acknowledge in particular the support of Austrian Federal Ministry of Science and Traffics, GZ 616.364/2-III/2a/98, FNRS–FWO, Belgium, FINEP, CNPq, CAPES, FUJB and FAPERJ, Brazil, Czech Ministry of Industry and Trade, GA CR 202/96/0450 and GA AVCR A1010521, Danish Natural Research Council, Commission of the European Communities (DG XII), Direction des Sciences de la Matière, CEA, France, Bundesministerium für Bildung, Wissenschaft, Forschung und Technologie, Germany, General Secretariat for Research and Technology, Greece, National Science Foundation (NWO) and Foundation for Research on Matter (FOM), The Netherlands, Norwegian Research Council, State Committee for Scientific Research, Poland, 2P03B06015, 2P03B1116 and SPUB/P03/178/98, JNICT–Junta Nacional de Investigação Científica e Tecnológica, Portugal, Vedecka grantova agentura MS SR, Slovakia, Nr. 95/5195/134, Ministry of Science and Technology of the Republic of Slovenia, CICYT, Spain, AEN96–1661 and AEN96-1681, The Swedish Natural Science Research Council, Particle Physics and Astronomy Research Council, UK, Department of Energy, USA, DE–FG02–94ER40817.

References

1. T. Sjöstrand, Comp. Phys. Comm. **82** (1994) 74
2. V.A. Khoze and W. Ochs, Int. J. Mod. Phys. **A12** (1997) 2949
3. Y.I. Azimov et al., Z. Phys. **C27** (1985) 65 and ibid. **C31** (1986) 213
4. A.H. Mueller, in Proc. 1981 Intern. Symp. on Lepton and Photon Interactions at High Energies ed. W.Pfeil (Bonn 1981) 689; Yu.L. Dokshitzer, V.S.Fadin and V.A. Khoze, Phys. Lett. **B115** (1982) 242
5. Yu.L. Dokshitzer, V.A. Khoze and S.I. Troyan, Int. J. Mod. Phys. **A7** (1992) 1875
6. C.P. Fong and B.R. Webber, Phys. Lett. **B229** (1989) 289
7. T. Sjöstrand and V.A. Khoze, Z. Phys. **C62** (1994) 281
8. G. Gustafson and J. Häkkinen, Z. Phys. **C64** (1994) 659
9. B.R. Webber, "QCD Event Generators", in "Physics at LEP2", eds. G. Altarelli, T. Sjöstrand and F. Zwirner, CERN 96-01 Vol 2 (1996) 161
10. J. Ellis and K. Geiger, Phys. Lett. **B404** (1997) 230
11. L. Lönnblad and T. Sjöstrand, Phys. Lett. **B351** (1995) 293
12. V. Kartvelishvili, R. Kvatadze and R. Möller, Phys. Lett. **B408** (1997) 331
13. V. Khoze et al., in "Physics at LEP2", eds. G. Altarelli, T. Sjöstrand and F. Zwirner, CERN 96-01 Vol 1 (1996) 190
14. A. Ballestrero et al., J. Phys. G: Nucl. Part. Phys. **24** (1998) 365
15. T. Sjöstrand and V.A. Khoze, Eur. Phys. J. **C6** (1999) 271
16. L. Lönnblad, Comp. Phys. Comm. **71** (1992) 15
17. G. Marchesini et al., Comp. Phys. Comm. **67** (1992) 465
18. DELPHI Coll., P. Abreu et al., Phys. Lett. **B462** (1999) 410
19. P. de Jong, in XXXth Int. Conference on High Energy Physics, Osaka (Japan) July/August 2000
20. V. Khoze and T. Sjöstrand, "QCD Interconnection Effects", in Proc. International Workshop on Linear Colliders, Sitges, Spain, April 28 - May 5, 1999, World Scientific, also LU-TP-99-23 (hep-ph/9908408)
21. K. Fialkovski and R. Wit, Nucl. Phys. **B** (Proc. Suppl.) **71** (1999) 187
22. A. De Angelis, Nucl. Phys. **B** (Proc. Suppl.) **71** (1999) 170
23. N. Watson, in Proc. of the XXIXth International Conference on High Energy Physics, Eds. A. Astbury, D. Axen and J. Robinson, Vancouver BC, Canada, July 1998, p. 499, also hep-ph/9809564
24. R. Möller, in Proc. of the XXIXth International Conference on High Energy Physics, Eds. A. Astbury, D. Axen and J. Robinson, Vancouver BC, Canada, July 1998, p. 504, also DELPHI note 98-167 PHYS 807
25. DELPHI Coll., P. Abreu et al., Nucl. Instr. Meth.**A303** (1991) 233
26. DELPHI Coll., P. Abreu et al., Nucl. Instr. Meth.**A378** (1996) 57
27. DELPHI Coll., P. Abreu et al., Z. Phys. **C77** (1996) 11
28. F. Berends et al., Comp. Phys. Comm. **85** (1995) 437
29. Particle Data Group, C. Caso et al., Eur. Phys. J. **C3** (1998) 1
30. P. Abreu et al., Nucl. Instrum. Meth. **A427** (1999) 487
31. S. Bethke et al., Nucl. Phys. **B370** (1992) 310
32. Yu.L. Dokshitzer, Phys. Lett. **B305** (1993) 295; P. Nason and B.R. Webber, in "Physics at LEP2", eds. G. Altarelli, T. Sjöstrand and F. Zwirner, CERN 96-01 Vol 1 (1996) 256
33. DELPHI Coll., P. Abreu et al., Phys. Lett. **B456** (1999) 310
34. DELPHI Coll., P. Abreu et al., Eur. Phys. J. **C5** (1998) 585
35. DELPHI Coll., P. Abreu et al., Z. Phys. **C65** (1995) 587
36. DELPHI Coll., P. Abreu et al., Phys. Lett. **B318** (1993) 249
37. N.C. Brummer, Z. Phys. **C66** (1995) 367
38. DELPHI Coll., P. Abreu et al., Phys. Lett. **B479** (2000) 89
39. JADE Coll., W.Bartel et al., Z. Phys. **C20** (1983) 187; *ibid.*, Phys. Lett. **B88** (1979) 171
40. PLUTO Coll., Ch. Berger et al., Phys. Lett. **B95** (1980) 313
41. MARK II Coll., P. C. Rowson et al., Phys. Rev. Lett. **54** (1985) 2580
42. TASSO Coll., W. Braunschweig et al., Z. Phys. **C45** (1989) 193
43. HRS Coll., M. Derrick et al., Phys. Rev. **D34** (1987) 3304
44. AMY Coll., H. Zheng et al., Phys. Rev. **D42** (1990) 737
45. DELPHI Coll., P. Abreu et al., Z. Phys. **C70** (1996) 179
46. ALEPH Coll., D. Busculic et al., Z. Phys. **C73** (1997) 409
47. DELPHI Coll., P. Abreu et al., Phys. Lett. **B372** (1996) 172
48. DELPHI Coll., P. Abreu et al., Phys. Lett. **B416** (1998) 233
49. L3 Coll., M. Acciarri et al., Phys. Lett. **B371** (1996) 137
50. L3 Coll., M. Acciarri et al., Phys. Lett. **B404** (1997) 390
51. L3 Coll., M. Acciarri et al., Phys. Lett. **B444** (1998) 569
52. OPAL Coll., G. Alexander et al., Z. Phys. **C72** (1996) 191
53. OPAL Coll., K. Ackerstaff et al., Z. Phys. **C75** (1997) 193
54. OPAL Coll., K. Ackerstaff et al., CERN-EP/99-178 (submitted to Eur. Phys. J. C)
55. A. De Angelis, in Proc. EPS-HEP Conference, Bruxelles 1995, p.63, Eds. J. Lemmone, C. Vander Velde, F. Verbeure (World Scientific, Singapore, 1996)
56. B.R. Webber, Phys. Lett. **B143** (1984) 501 and references therein
57. Z. Koba et al., Nucl. Phys. **B40** (1972) 317
58. B. R. Webber, "QCD Cascade Approach to Jet Fragmentation", in Proc. XV Int. Symp. on Multiparticle Dynamics, Lund 1984, Eds. G. Gustafson and C. Peterson (World Scientific, Singapore, 1984)
59. OPAL Coll., G. Abbiendi et al., Phys. Lett. **B453** (1999) 153; OPAL Coll., K. Ackerstaff et al., Eur. Phys. J. **C1** (1998) 395